Functionalized resorcinarenes effectively disrupt the aggregation of αA66−80 crystallin peptide related to cataracts

Kwaku Twum,[a] Avik Bhattacharjee,[b] Erving T. Laryea,[a] Josephine Esposto,[c] Shaelyn Mortensen,[c] George Omolloh[b], Maya Jaradi,[a] Naomi L. Stock,[d] Nicholas Schileru,[a,e] Bianca Elias,[a] Elan Pszenica[a], Theresa McCormick,[b] Sanela Martic,*[c,d] Ngong Kodiah Beyeh*[a]

[a] Department of Chemistry, Oakland University, 146 Library Drive, Rochester, MI 48309-4479, USA.
[b] Department of Chemistry, Portland State University, Oregon, USA.
[c] Department of Forensic Science and Environmental and Life Sciences Program, Water Quality Center, Trent University, ON, Canada, K9L0G2.
[d]Water Quality Centre, Trent University ON, Canada K9L 0G2
[e]Department of Osteopathic Medicine, Midwestern University, 555 31st St., Downers Grove, IL 60515, USA.

Supporting Information

Table of Contents

I. General Information

The receptors **A**, **B** and **C** were synthesized according to reported procedures.[1–3] The αA66-80 crystallin peptide was purchased from GenScript. All the solvents used were purchased from Thermo Fisher Scientific and Sigma Aldrich, USA. Fluorescence Proteostat aggregation and dynamic light scattering experiments were carried out in 10mM TRIS buffer using TAKE 3 BioTek microplate reader and Malvern ZetaSizer Nano respectively. ^{1}H NMR and ESI-mass spectrometry were carried out on 400MHz Bruker Spectrometer and Thermo Fisher Scientific QExactive Orbitrap, respectively.

II. Proteostat Aggregation Assay

Receptor:peptide concentrations were prepared by pipetting 10uL of 5360 µM freshly prepared crystallin peptide solution in 10mM Tris buffer. 1 μL of a more concentrated solution of the receptor is added to the solution to make 0.2:1, 0.4:1, 0.6:1, 0.8:1, 1:1, 5:1 and 10:1 ratio that is then incubated at 37°C for 7 days. A control sample of peptide alone was also incubated for same duration. After the incubation period, a 1 μL aliquot of proteostat dye is added into 10 μL of each sample solution. Prior to transferring each sample into the microplate wells, positive and negative controls were prepared and added to the plate in order to ensure sample integrity and to verify that there was minimal contribution of free proteostat dye solution to the level of fluorescence intensity measured. Fluorescence readings were done at 25 °C, emission of 550 nM and excitation of 600 nM to monitor the extent of fibrils and filaments formed. All the measurements were done in triplicates

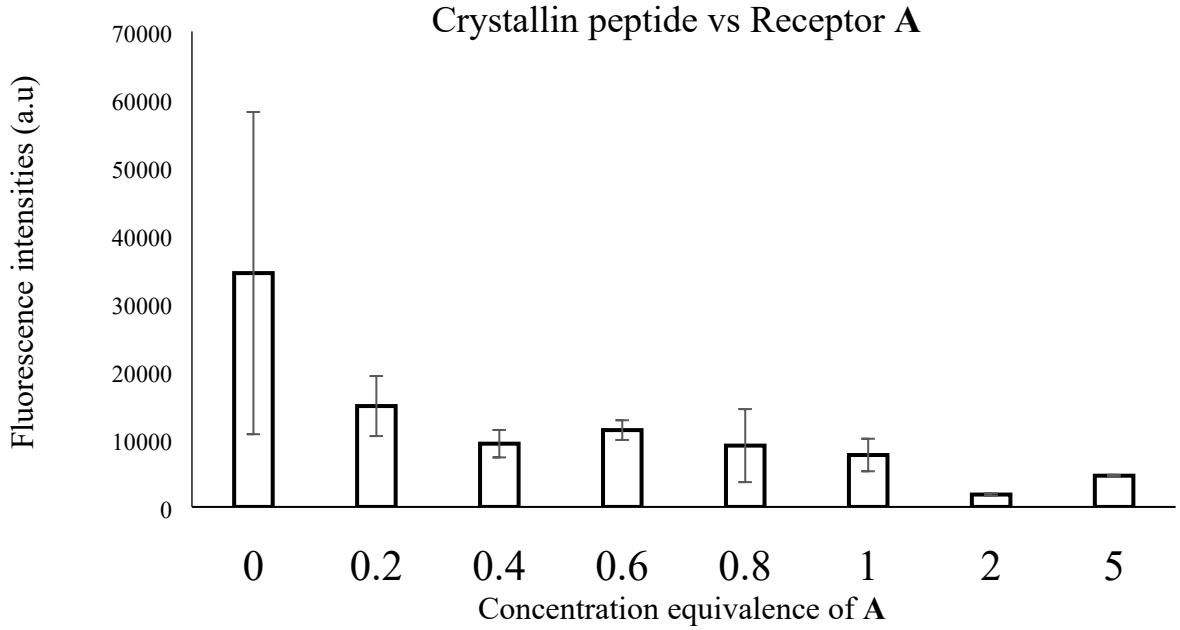

Figure S1. Bar chart of fluorescence different concentration ratio of receptor **A** into 1 equivalence of αA66-80 crystallin peptide. Error bars are the standard deviations of the mean of triplicate measurements.

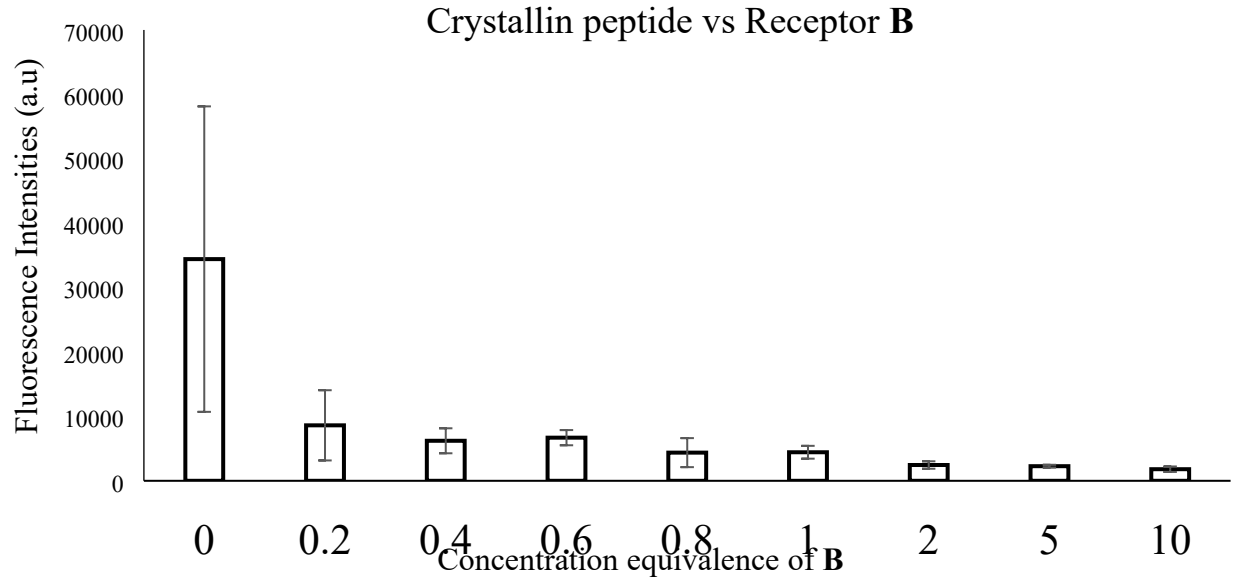

Figure S2. Bar chart of fluorescence different concentration ratio of receptor **B** into 1 equivalence of αA66-80 crystallin peptide. Error bars are the standard deviations of the mean of triplicate measurements.

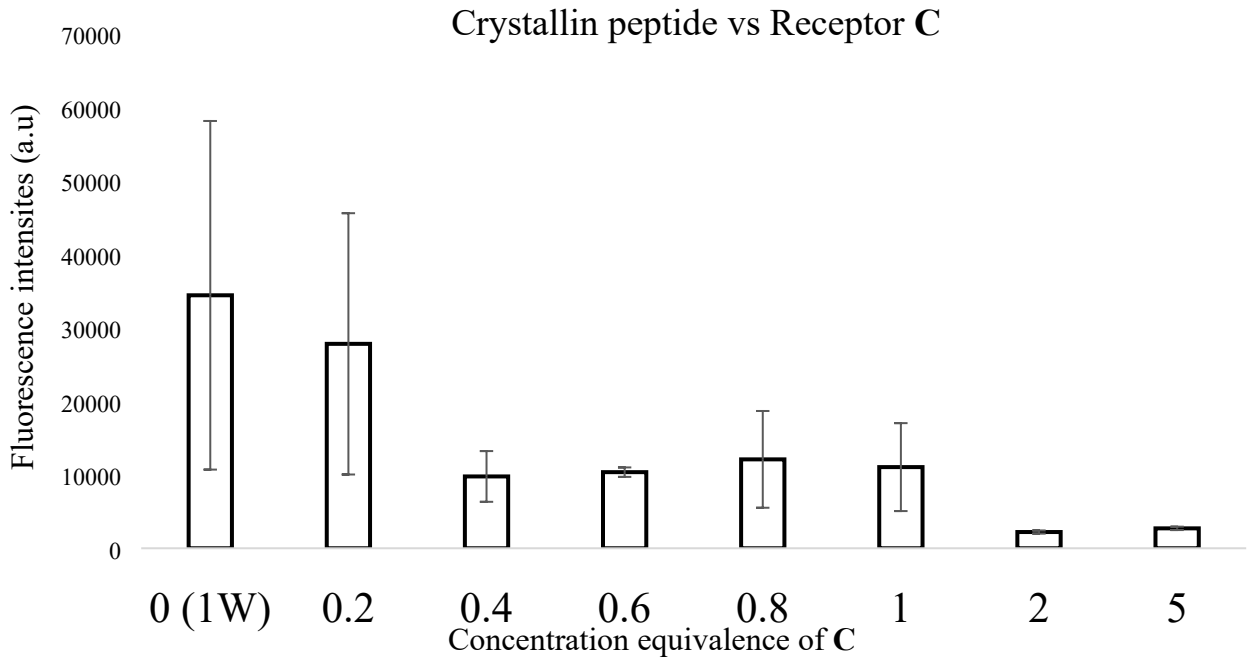

Figure S3. Bar chart of fluorescence different concentration ratio of receptor **C** into 1 equivalence of αA66-80 crystallin peptide. Error bars are the standard deviations of the mean of triplicate measurements.

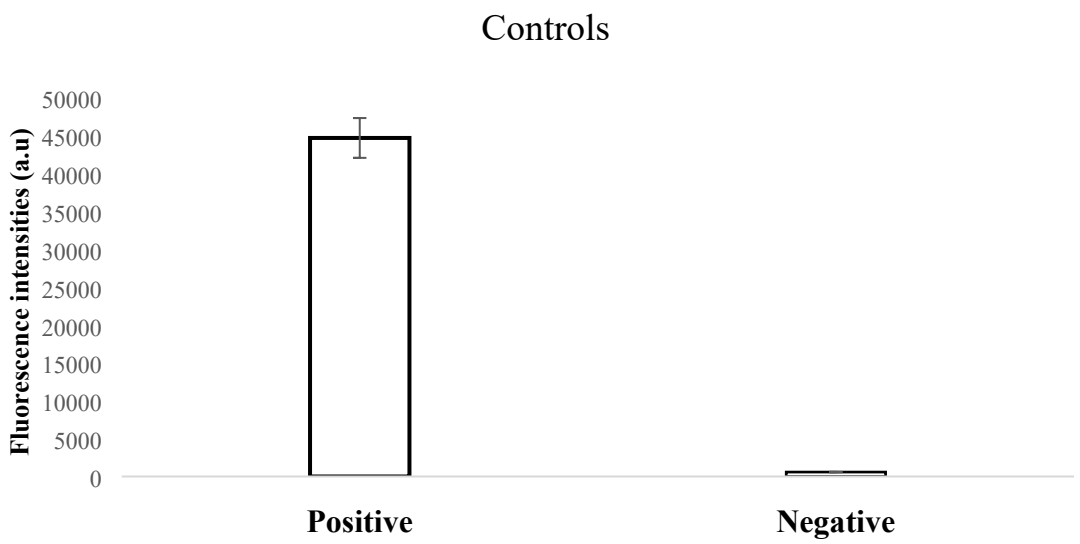

Figure S4. Bar chart of fluorescence intensities of positive and negative controls of the Proteostat dye. Error bars are the standard deviations of the mean of triplicate measurements.

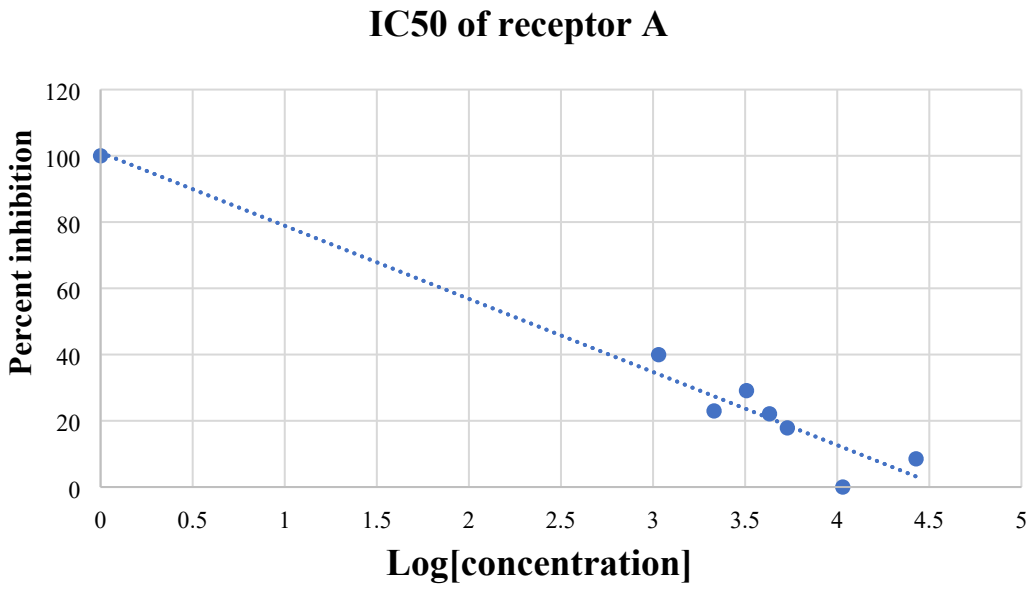

Figure S5. Plot of percent inhibition vs log[concentration] from fluorescence aggregation assay of receptor **A** vs αA66-80 crystallin peptide.

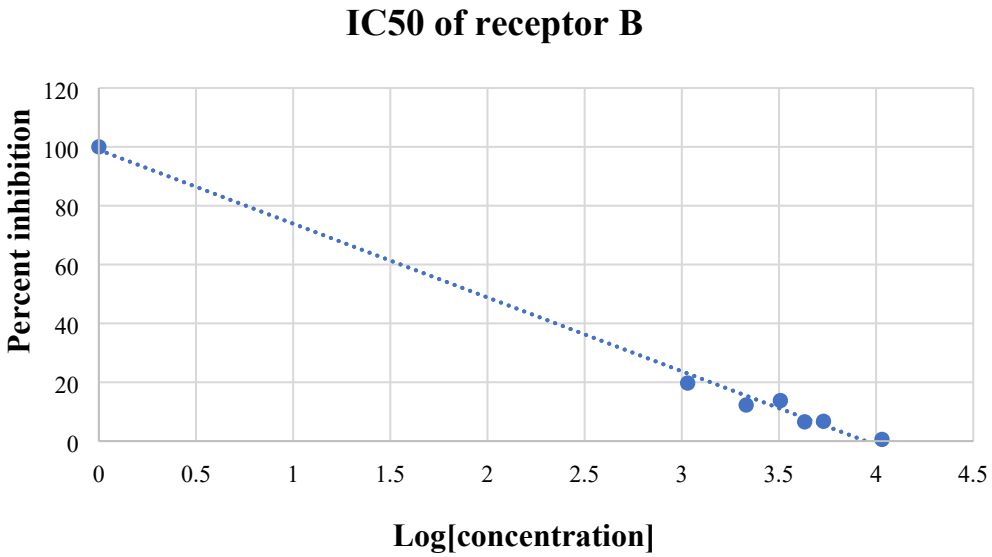

Figure S6. Plot of percent inhibition vs log[concentration] from fluorescence aggregation assay of receptor **B** vs αA66-80 crystallin peptide.

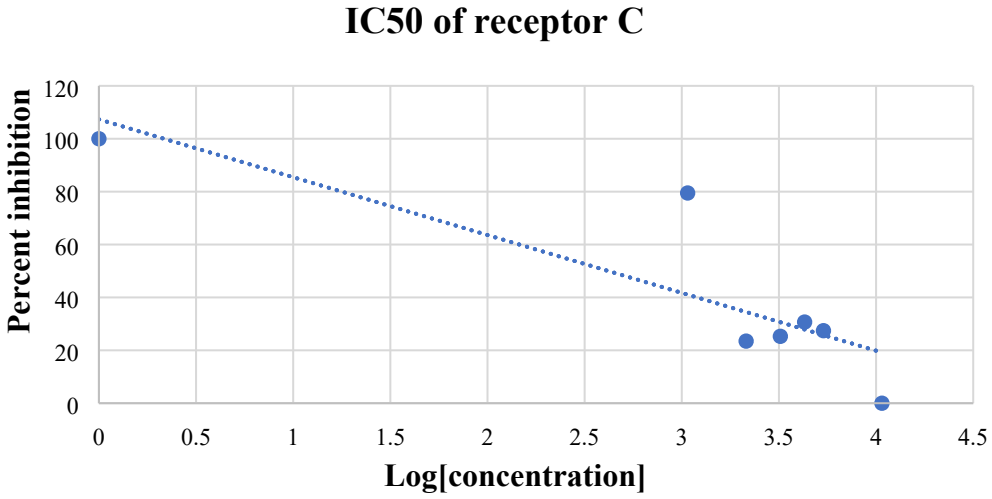

Figure S7. Plot of percent inhibition vs log[concentration] from fluorescence aggregation assay of receptor **C** vs αA66-80 crystallin peptide.

III. Dynamic Light Scattering (DLS) Experiments

Receptor:peptide concentrations were prepared by pipetting 50 μL of freshly prepared crystallin solution in 10 mM Tris buffer. 1 μL of a more concentrated solution of the receptor is added to the solution to make 0.2:1, 0.4:1, 0.6:1, 0.8:1, 1:1, 5:1 and 10:1 ratio that is then incubated at 37°C for 7 days. A control sample of peptide alone was also incubated for same duration. After the incubation period, 50 μL of the prepared sample is pipetted into a Malvern's microvolume cuvette

appropriate for light scattering experiment. DLS measurements are collected in triplicates and averaged for a sample solution.

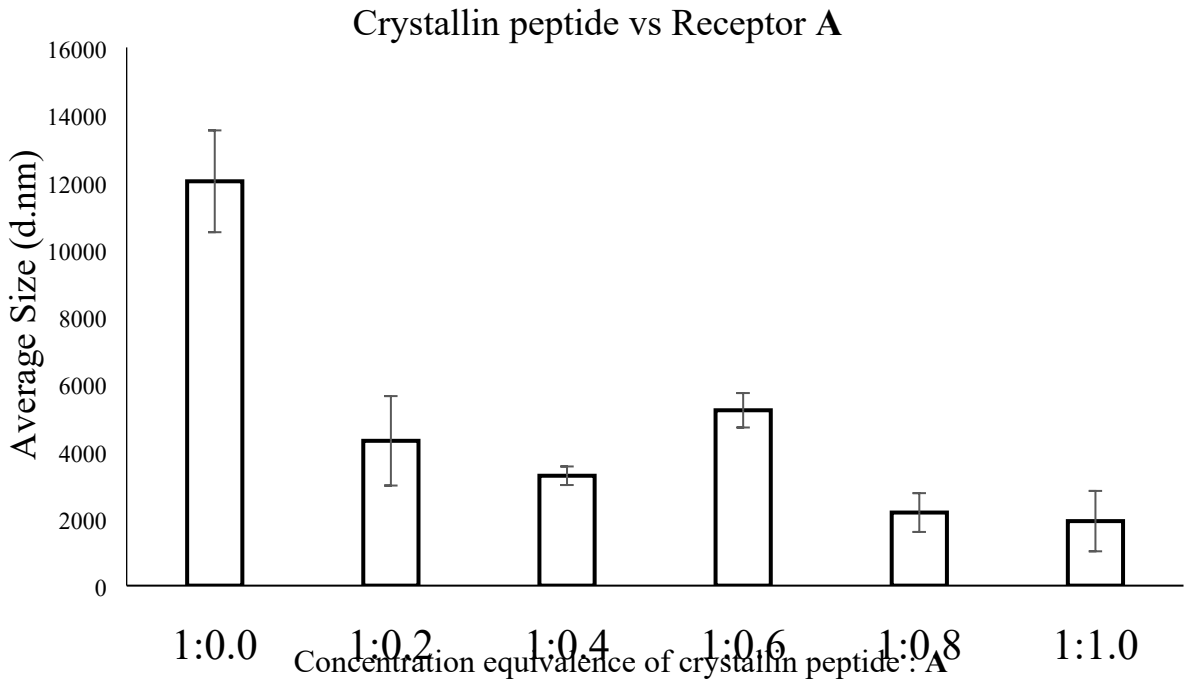

Figure S8. Bar chart of Z-average size (d.nm) different concentration ratio of receptor **A** into 1 equivalence of αA66-80 crystallin peptide. Error bars are the standard deviations of the mean of triplicate measurements.

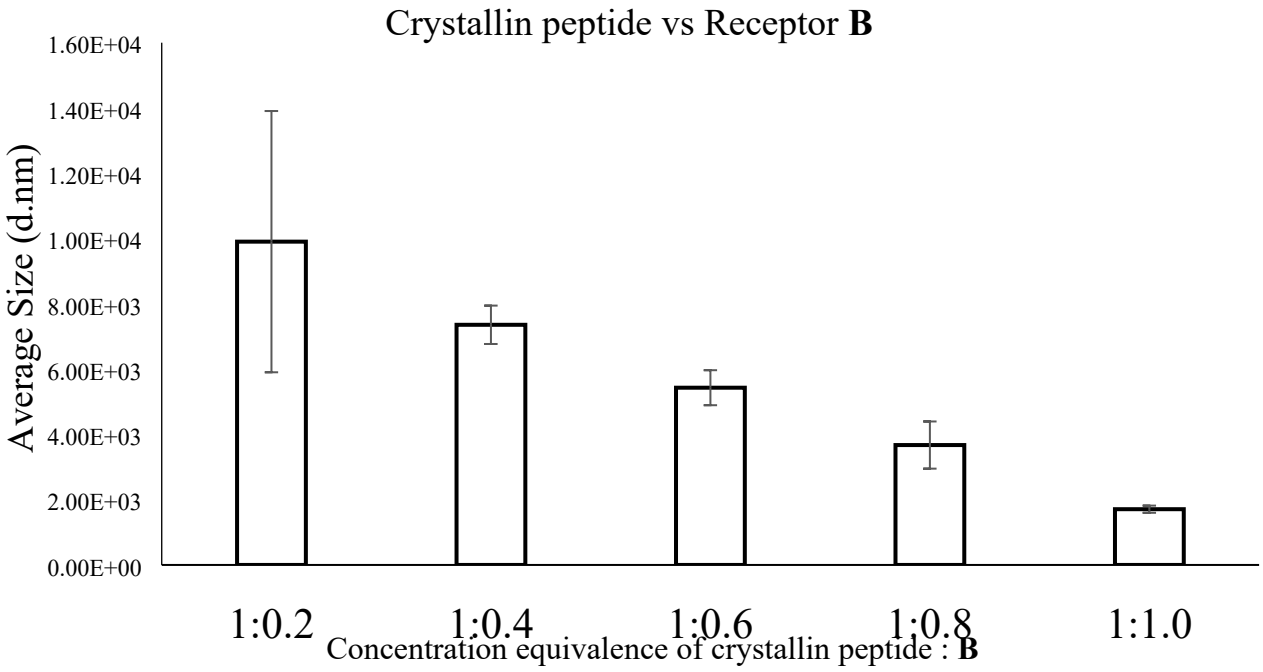

Figure S9. Bar chart of Z-average size (d.nm) of different concentration ratio of receptor **B** into 1 equivalence of αA66-80 crystallin peptide. Error bars are the standard deviations of the mean of triplicate measurements.

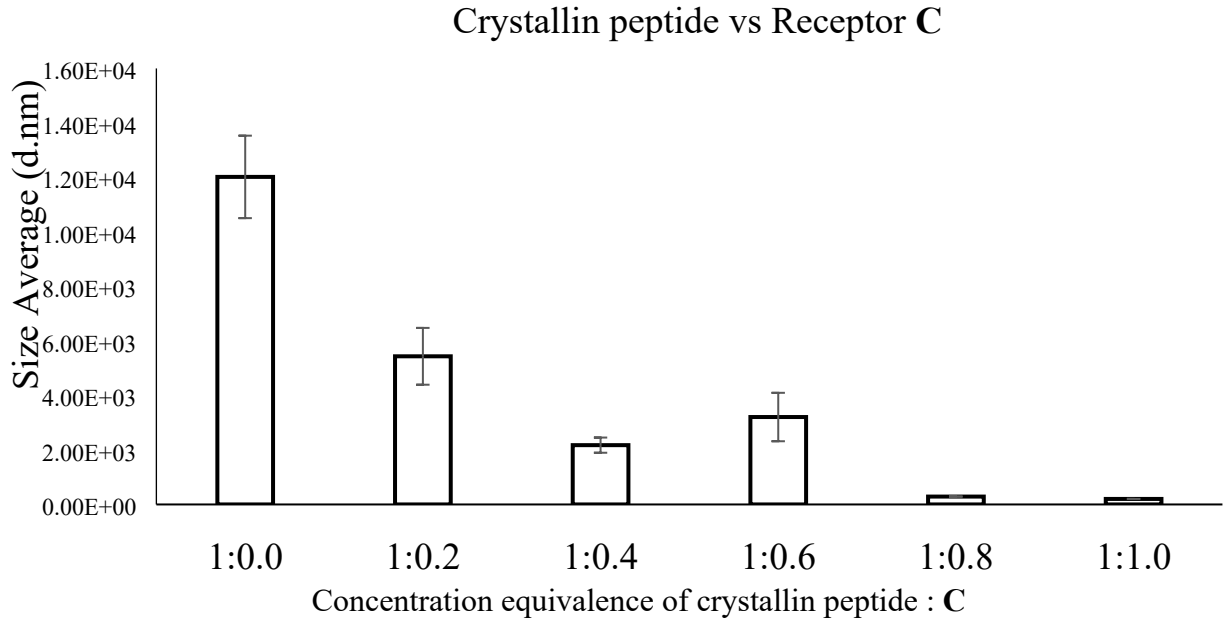

Figure S10. Bar chart of Z-average size (d.nm) of different concentration ratio of receptor **C** into 1 equivalence of αA66-80 crystallin peptide. Error bars are the standard deviations of the mean of triplicate measurements.

IV. Transmission Electron Microscopy (TEM) Imaging

αA66-88 crystalline peptide was aggregated in the presence of the receptors in the concentration ratio of 1:1 and 5:1. Pure crystallin was also prepared and stained without aggregation. Samples were incubated for 7 days at 37 ^{o}C. 10 µL aliquots were taken from each sample on day 7. The samples were then loaded onto a Formvar-carbon coated 200 mesh nickel grids and allowed to absorb for 2 hours in ambient light. The grids were washed with 1 mL deionized water three times and blotted dry. 2% glutaraldehyde solution was then loaded onto each grid for 5 minutes. The addition of glutaraldehyde stabilized the surface of the grid as well as the aggregates formed for imaging. The grids were washed again with 1 mL deionized water three times, after which the grids were blotted dry. After the stabilization of the surface of the grids with glutaraldehyde, 1 % Uranyl Acetate solution was loaded onto the surface of the grids for 5 minutes. Uranyl acetate induced the needed electron density for imaging as well as stained the background of the grid for easy identification of aggregates. The grids were finally washed with 1 mL deionized water three times. Images from the TEM were taken at 22000x, 56000x, and 140000x magnification to obtain an overall evaluation of the samples. Duplicate grids were made for each sample.

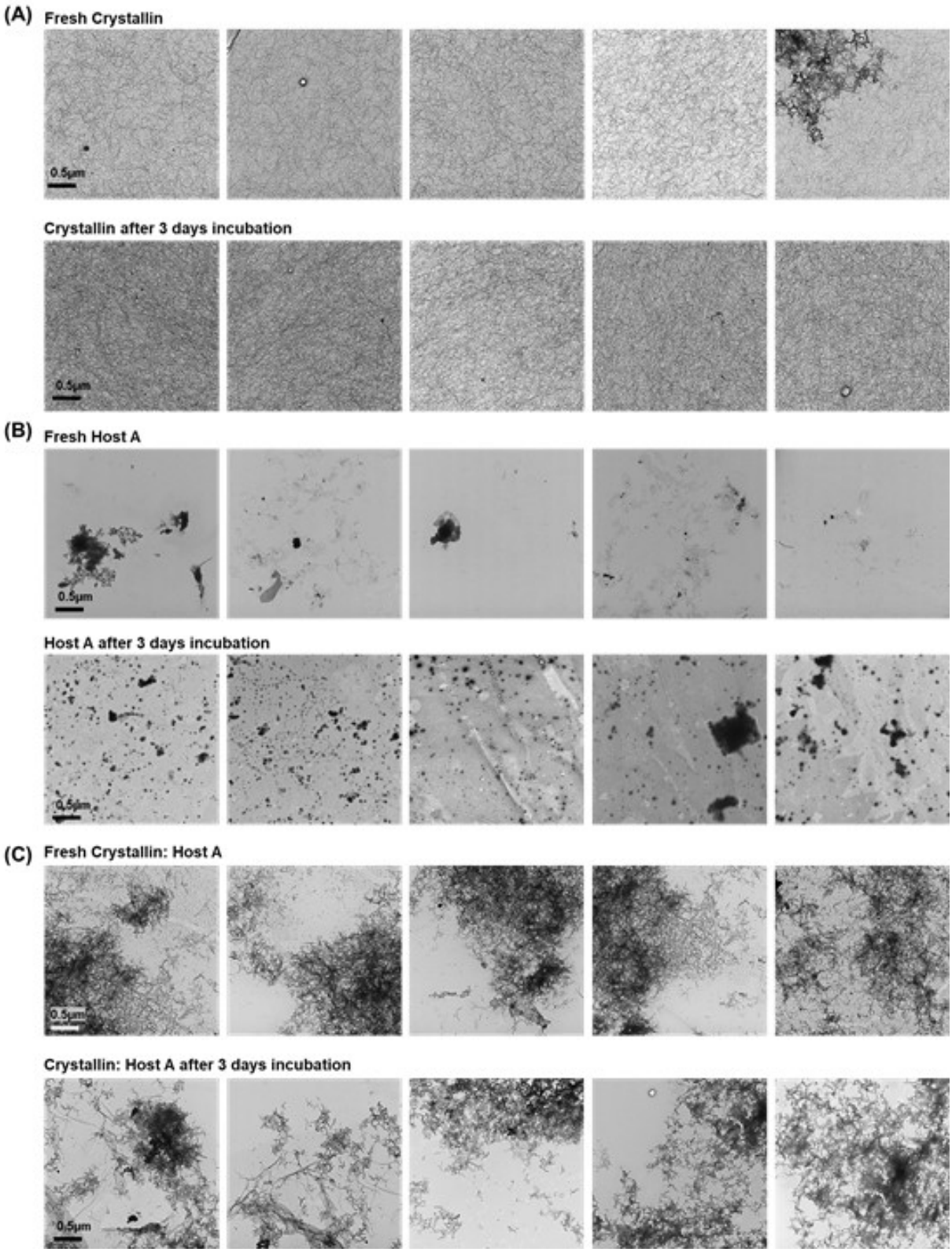

Figure S11. TEM images of α66-80 fresh (t = 0) and aged (t = 3 days) (A) crystallin peptide alone, (B) receptor **A** alone, and (C) crystallin:receptor **A** complex (1:1 concentration ratio) after 3 days incubation.

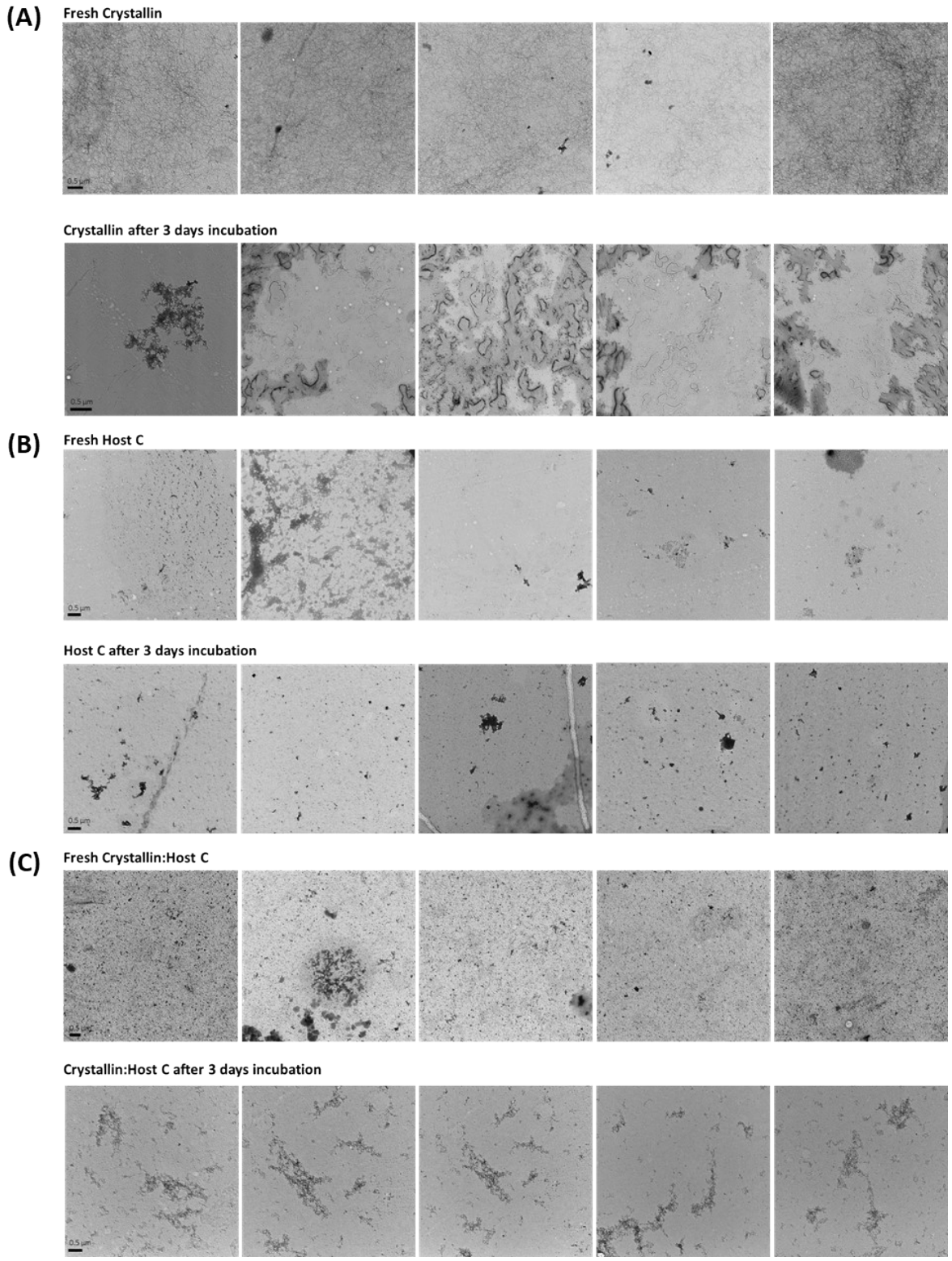

Figure S12. TEM images of α66-80 fresh (t = 0) and aged (t = 3) (A) crystallin peptide alone, (B) receptor **C** alone, and (C) crystallin:receptor **C** complex (1:1 concentration ratio) after 3 days incubation.

V. Mass Spectrometry

Mass spectrometry of host-guest complexes

All receptors/hosts (**A**, **B** and **C**) and α66-80 crystallin peptide were successfully identified by ESI-MS. The complexes formed by α66-80 crystallin peptide with Host **A** and **B** were evident in MS, and no complexes were formed with Host **C**.

V.I. Solution preparation

A 10 mM stock solution of the α66-80 crystallin peptide in water was prepared from 5 mg of solid α66-80 crystallin peptide. The solution was stored in 40 mL aliquots at -80 ^{o}C. 10 mM stock solutions of both host **A** and host **B** were also prepared from 5 mg of solid powder in water. The host solutions were stored in 20 mL aliquots at -20 ^{o}C.

For analysis of each molecule individually, 50 µM solutions were prepared by combining 5 mL of the 10 mM stock solutions with 955 mL of the ESI buffer in a microcentrifuge tube and vortexing for 1 minute. The ESI buffer consisted of 50% HPLC grade methanol, 49% water and 1% acetic acid (%v).

For complexation studies, equal parts of 10 mM peptide and 10 mM host (either **A** or **B**) were combined in a microcentrifuge tube, vortexed for 1 min and briefly centrifuged down. This yielded equimolar (5 mM: 5 mM) host-peptide mixes. 2 mL were immediately portioned out into a separate centrifuge tube with 198 mL ESI buffer to dilute the concentration of each to 50 mM. This sample was analyzed with ESI-MS immediately, within 2 hours of preparing the solution. The remaining solution was incubated for 72+ hours at 37 ^{o}C. After incubation, the samples were diluted 100 times in ESI buffer to give a 50 mM: 50 mM (host: peptide) solution. After dilution, the samples were analyzed with ESI-MS within the following 2 hours.

V.II. Mass spectrometry instrument and parameters

An Orbitrap Q-Exactive mass spectrometer (Thermo Fisher Scientific, San Jose, CA) equipped with an electrospray ionization (ESI) source was used to analyze all samples. Samples were analyzed in positive ion mode with a sample flow rate of 10 µL/min. The capillary voltage was set to 4.00 kV with a nitrogen sheath gas flow rate of 5 arbitrary units. Capillary temperature on the ESI source was set to 40 ^{o}C. The instrument resolving power was set to 17,500. Spectra were captured with an acquisition time of 1 minute over the mass range of *m/z* 266.7 to 4,000 for mixtures and *m/z* 166.7 to 2500 for free sample solutions. Mass calibration using Pierce Calibration Solution (Thermo Fisher Scientific) was performed prior to analysis on each day samples were run for the corresponding ion mode that was used (positive). The spectra were analyzed using the Xcalibur Qual Browser (4.1) data processing software.

V.III. MS characterization of free peptide, and hosts

ESI-MS was used to characterize each host molecule and the peptide using freshly made sample solutions. Figure S13A shows a partial positive mode MS spectrum for the peptide, and the molecular ion peak at *m/z* 622.6646 $[M+3H]^{3+}$, associated with the triply charged peptide.

Figure S13B shows a positive mode mass spectrum for Host **A**, and the peak at *m/z* 1065.097 $[M+H]^{+}$, associated with singly charged protonated Host **A**. In addition, other singly charged ions were observed for the host including: $[M-3Na+4H]^{+}$ at *m/z* 999.1512, $[M-2Na+3H]^{+}$ at *m/z* 1021.1332, $[M-Na+2H]^{+}$ at *m/z* 1043.158, and $[M+Na]^{+}$ at *m/z* 1087.0782 (Table S1).

Host **B** was also characterized by MS and the obtained mass spectrum shows a singly charged $[M+H]^{+}$ ion peak at *m/z* 1009.0296 (Figure S13C). The following characteristic singly charged ions were also observed: $[M-3Na+4H]^{+}$ at *m/z* 943.0844, $[M-2Na+3H]^{+}$ at *m/z* 965.0672, $[M-Na+2H]^{+}$ at *m/z* 987.0481, and $[M+Na]^{+}$ at *m/z* 1031.0131 (Table S1). Host **C** was characterized by MS and was observed as a doubly charged ion with complete loss of chloride ions and the loss of 2 hydrogens, [Host **C**-2H-4Cl]$^{2+}$ at *m/z* 599.3110 (Figure S13D).

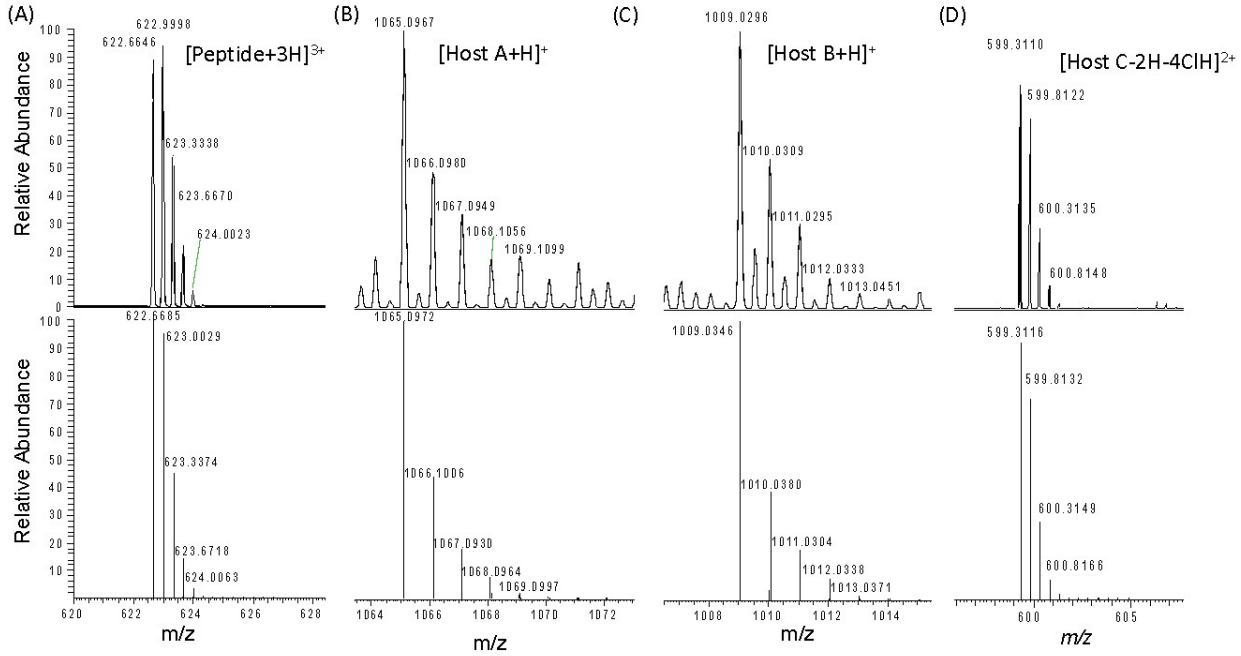

Figure S13. Positive mode ESI-MS spectra of (A) the α66-80 crystallin peptide, (B) Host **A**, (C) Host **B** and (D) Host **C** with their respective theoretical isotope distributions.

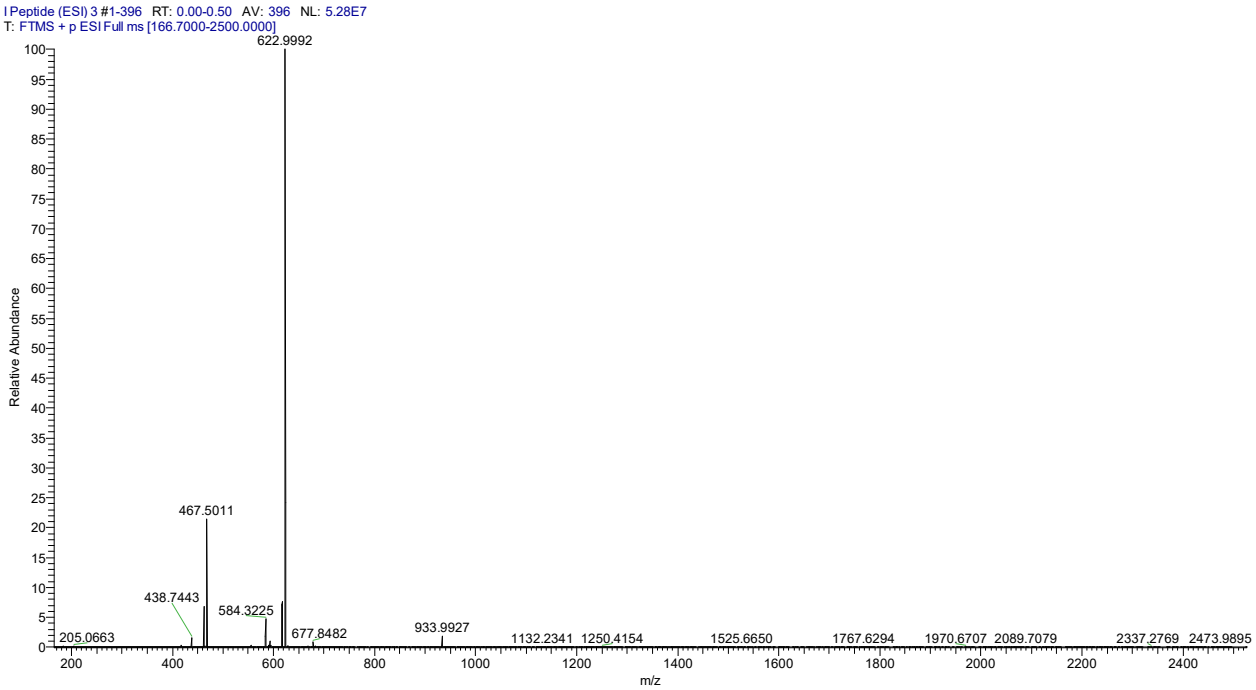

Figure S14. Positive mode ESI-MS spectra of crystallin peptide

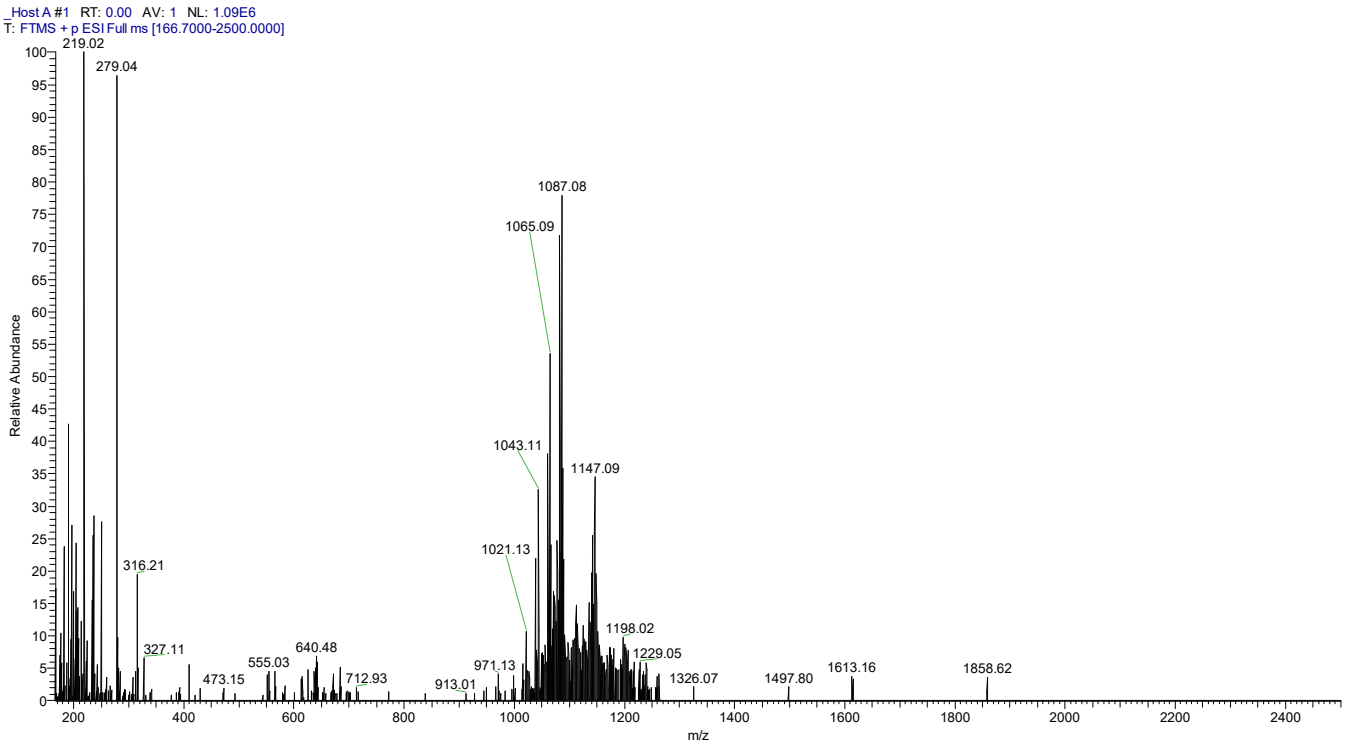

Figure S15. Positive mode ESI-MS spectra of receptor **A**.

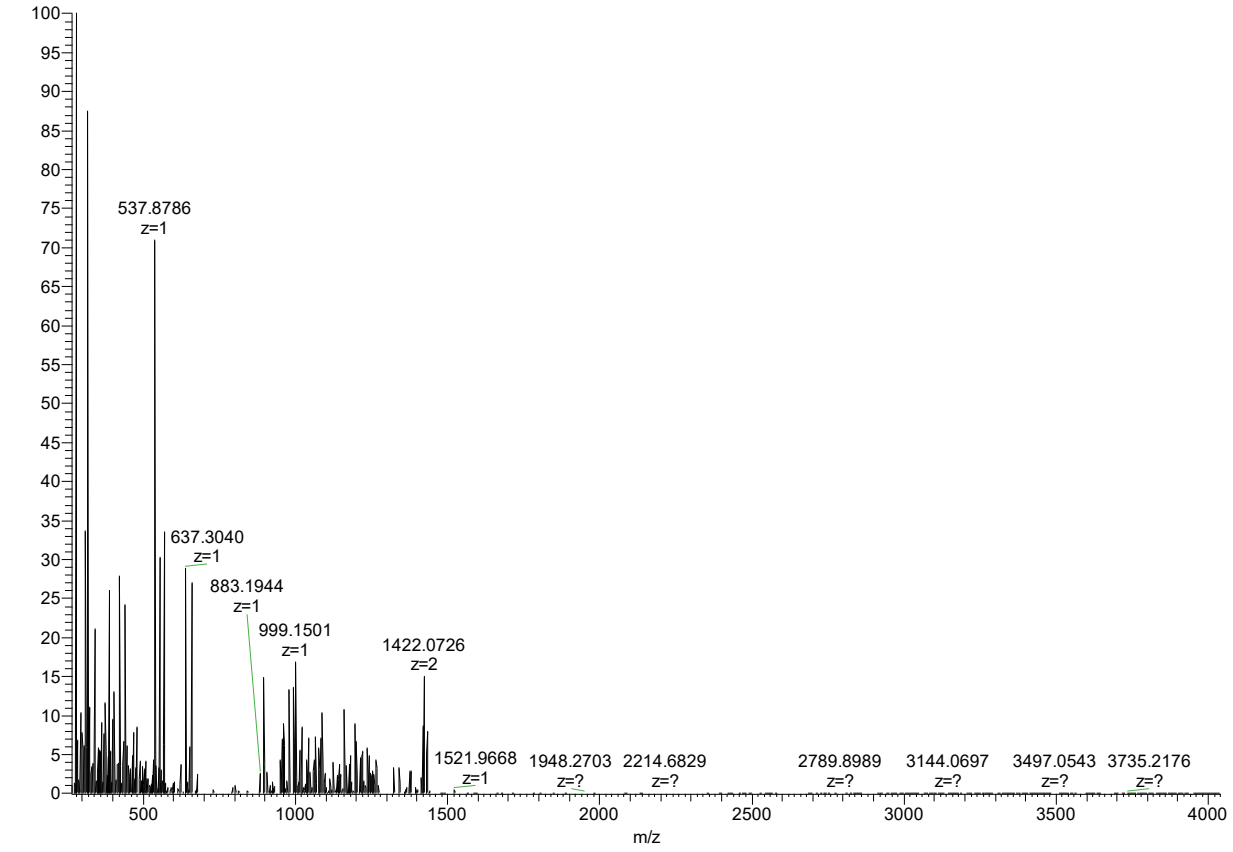

Figure S16. Positive mode ESI-MS spectra of receptor **A** + peptide.

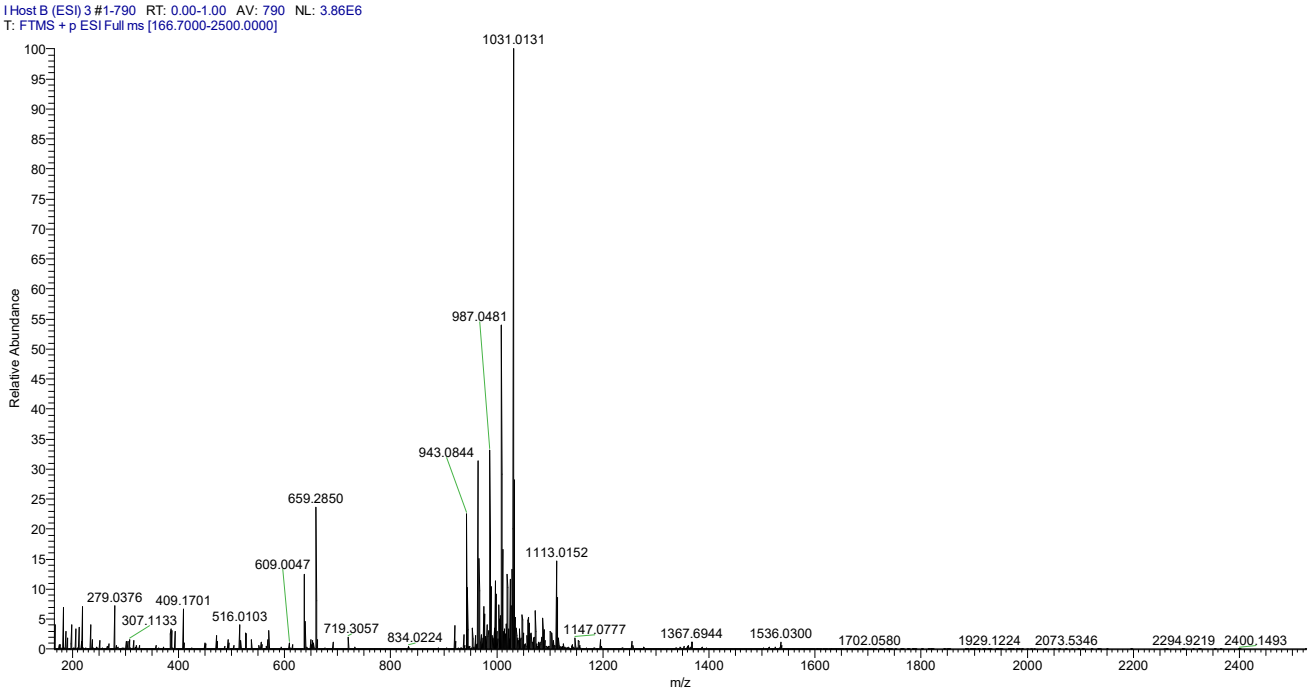

Figure S17. Positive mode ESI-MS spectra of receptor **B**.

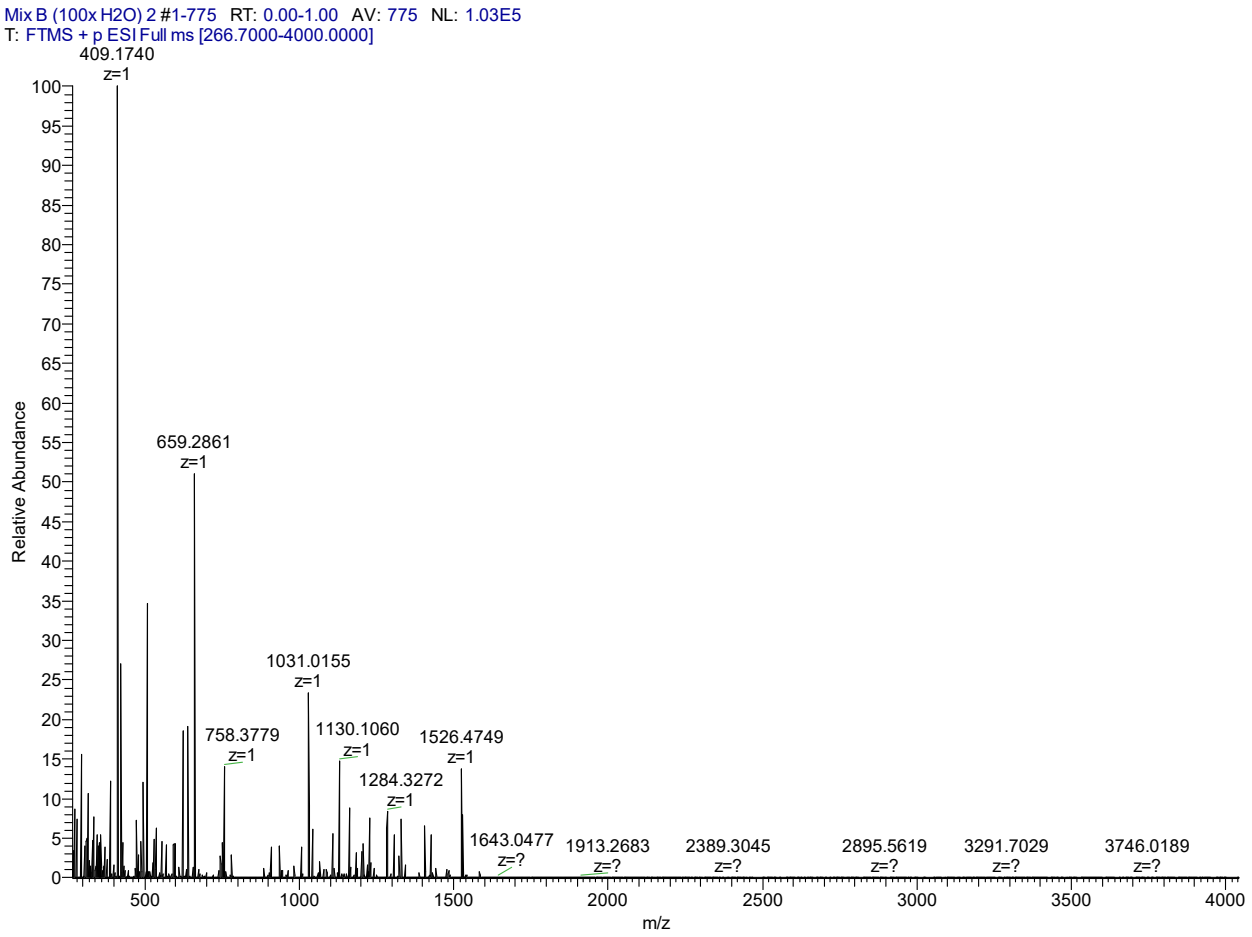

Figure S18. Positive mode ESI-MS spectra of receptor **B** + peptide.

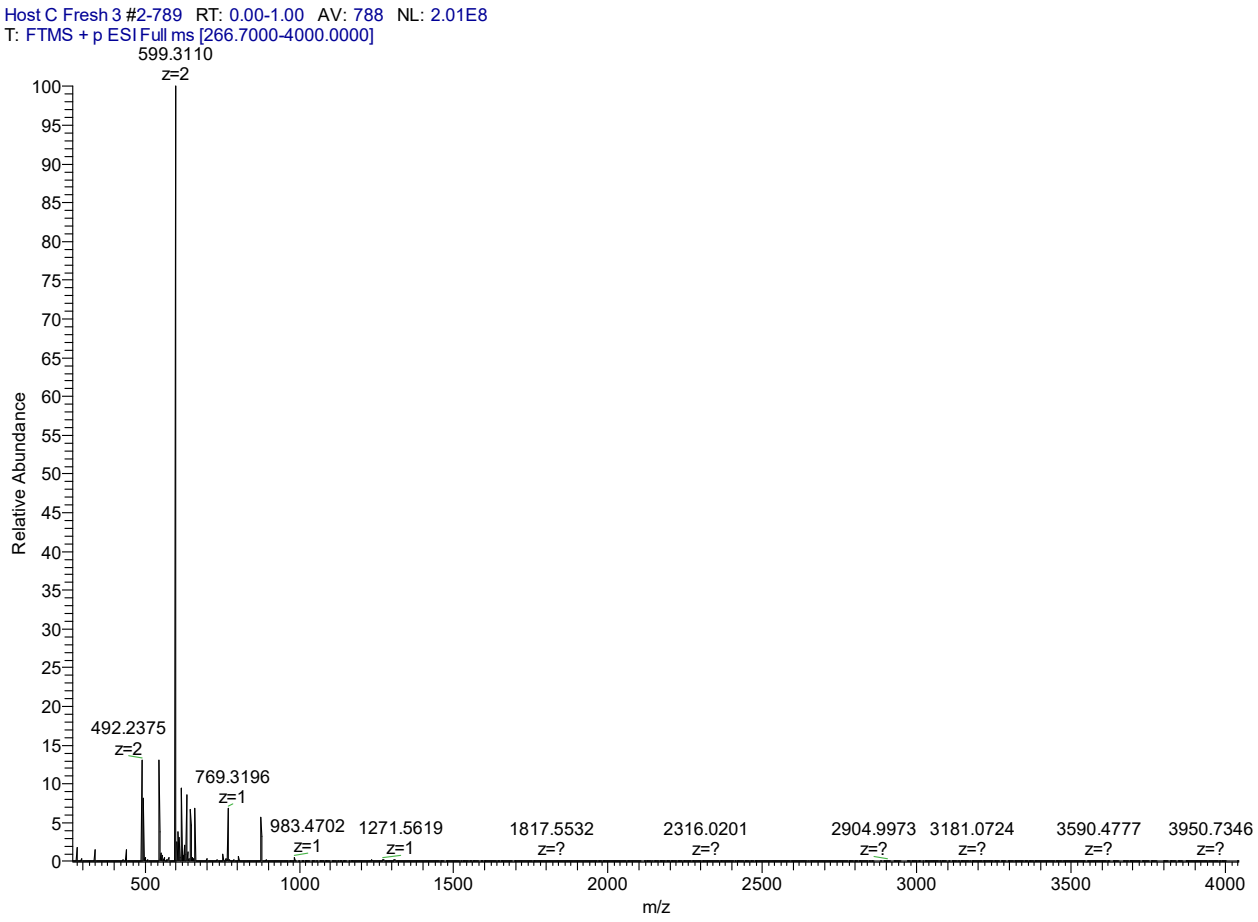

Figure S19. Positive mode ESI-MS spectra of receptor **C**.

Table S1. Theoretical and observed *m/z* values for select high relative abundance peaks in the peptide, host **A**, host **B** and host **C** spectra.

Ion	Observed *m/z*	Theoretical *m/z*
Peptide		
$[Peptide+4H]^{4+}$	467.2523	467.2532
$[Peptide+3H]^{3+}$	**622.6646**	**622.6685**
$[Peptide+2H]^{2+}$	933.4970	933.4964
Host A		
$[Host\ A\text{-}4Na+5H]^{+}$	977.1676	977.1695
$[Host\ A\text{-}4Na+4H+NH_4]^{+}$	994.1945	994.1960
$[Host\ A\text{-}3Na+4H]^{+}$	999.1512	999.1514
$[Host\ A\text{-}3Na+3H+NH_4]^{+}$	1016.1773	1016.1779
$[Host\ A\text{-}2Na+3H]^{+}$	1021.1332	1021.1333
$[Host\ A\text{-}2Na+2H+NH_4]^{+}$	1038.1583	1038.1599
$[Host\ A\text{-}Na+2H]^{+}$	1043.1158	1043.1153
$[Host\ A\text{-}Na+H+NH_4]^{+}$	1060.1373	1060.1418
$[Host\ A+H]^{+}$	**1065.0967**	**1065.0972**
$[Host\ A+NH_4]^{+}$	1082.1196	1082.1238
$[Host\ A+Na]^{+}$	1087.0786	1087.0792
$[Host\ A+MeOH+H]^{+}$	1097.1178	1097.1234
$[Host\ A+NaCH_3CO_2+H]^{+}$	1147.0751	1147.1003
Host B		
$[Host\ B\text{-}4Na+5H]^{+}$	921.1039	921.1069
$[Host\ B\text{-}3Na+4H]^{+}$	943.0844	943.0888
$[Host\ B\text{-}2Na+3H]^{+}$	965.0672	965.0707
$[Host\ B\text{-}Na+2H]^{+}$	987.0481	987.0527
$[Host\ B+H]^{+}$	**1009.0296**	**1009.0346**
$[Host\ B+Na]^{+}$	1031.0131	1031.0166
Host C		
$[Host\ C\text{-}4HCl+2H]^{2+}$	**599.3110**	**599.3116**
$[Host\ C\text{-}3HCl+H]^{2+}$	617.2983	617.2999
$[Host\ C\text{-}2HCl]^{2+}$	635.2862	635.2882
$[Host\ C\text{-}2HCl+H]^{+}$	1269.5778	1269.5692
$[Host\ C\text{-}HCl+H]^{+}$	1307.5479	1307.5429

V.IV. MS characterization of host-peptide complexes

In order to characterize host-peptide complexes, each host was co-mixed with the peptide in 1:1 equimolar amounts (50 mM: 50 mM) and analyzed by ESI-MS freshly or after incubated for 72 hours at 37 ^{o}C.

Figure S14 shows a positive mode ESI-MS spectrum of observed triply charged Host **A**-peptide complex peaks. The identification of each complex was achieved by comparing experimental with theoretical distribution. Four peaks associated with the triply charged complex were observed with increasing sodium loss and different adducts (Table S2). Peaks associated with free host **A** and the peptide (non-complexed) were also observed.

(A)

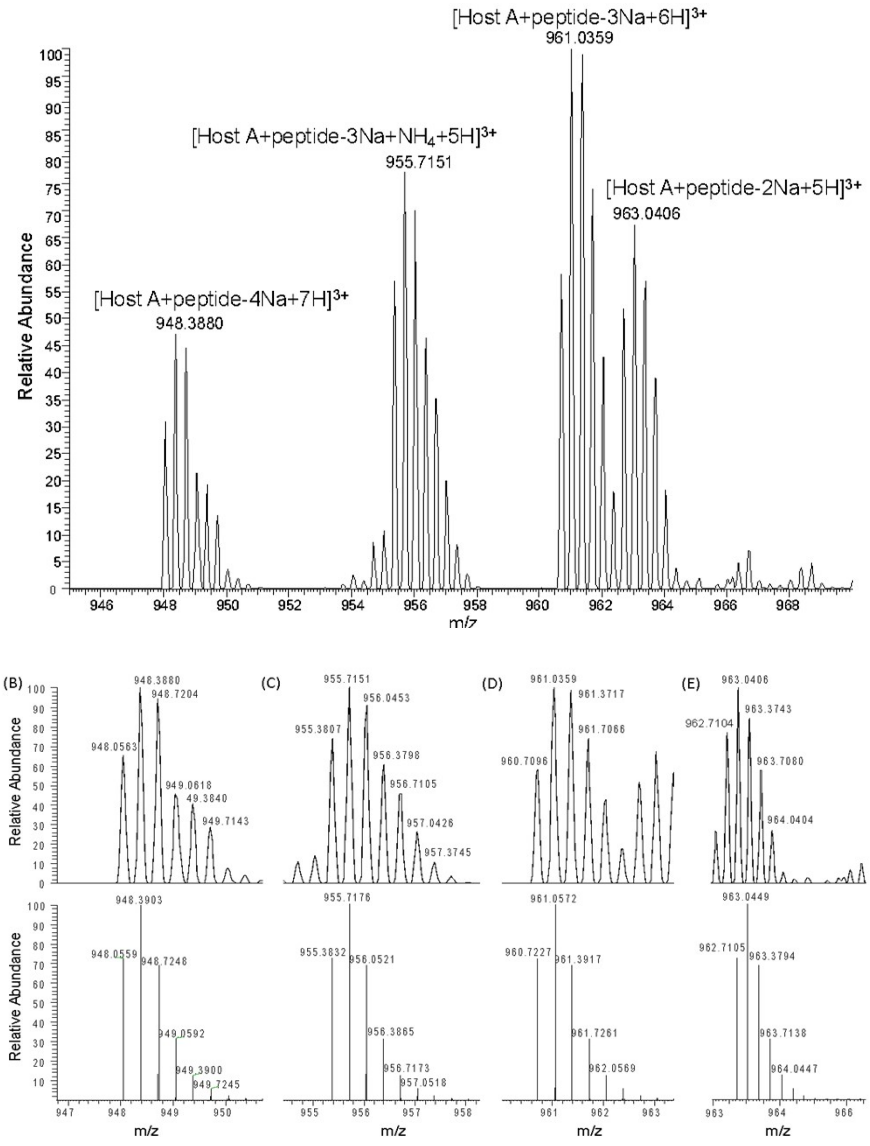

Figure S20. (A) A positive mode ESI-MS spectra of host **A**-peptide triply charged complexes and comparison with their respective theoretical isotope patterns for (B) [Host A+peptide-4Na+7H]$^{3+}$ (C) [Host A+peptide-3Na+NH_4+5H]$^{3+}$ (D) [Host A+peptide-3Na+6H]$^{3+}$ and (E) [Host A+peptide-2Na+5H]$^{3+}$

Table S2. Theoretical and observed *m/z* values for triply charged host **A** and peptide complexes

Ion	Observed m/z	Theoretical m/z
[Host+peptide-4Na+7H]$^{3+}$	948.3880	948.3903
[Host+peptide-3Na+NH_4+5H]$^{3+}$	955.7151	955.7176
[Host+peptide-3Na+6H]$^{3+}$	**961.0359**	**961.0572**
[Host+peptide-2Na+5H]$^{3+}$	963.0406	963.0449

Host **B**+peptide complexes were also observed as both triply and doubly charged ions. Figure S15 shows the MS spectrum of singly and triply charged complexes. Similar to host **A**, the host **B**+peptide complexes, the multiply charged ions are expected due to the multiple basic amino acids present in the peptide and the chosen ionization method. Additional data is presented in Table S3.

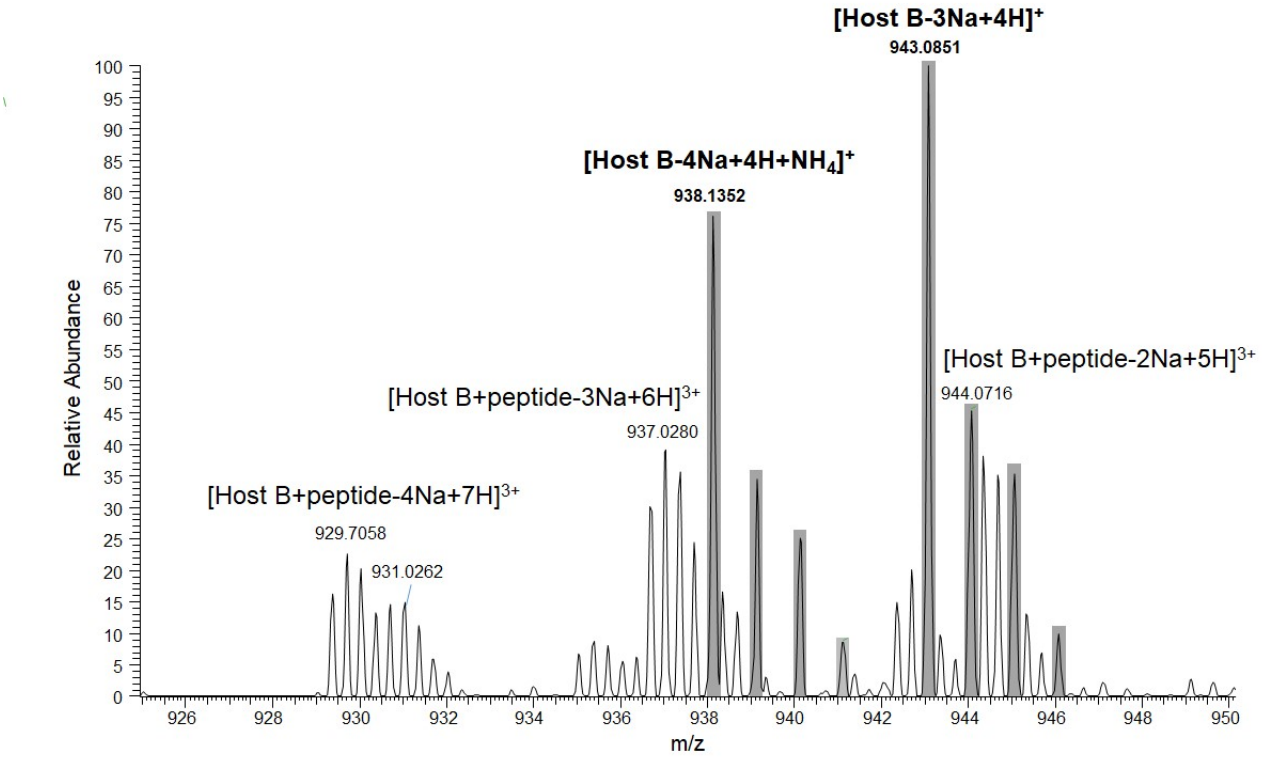

Figure S21. Partial positive mode ESI-MS spectrum of singly and triply charged Host B+peptide complexes showing proposed molecular ions peaks.

Table S3. Observed and theoretical *m/z* values for complex peaks and free host **B** peaks in the incubated host **B**+peptide mixture spectrum with calculated mass accuracies. Mass accuracy for [Host B+peptide-2Na+5H]3+ is calculated according to the second most abundant peak due to overlap with the isotope pattern for [Host B-3Na+4H]+.

Ion	Observed *m/z*	Theoretical *m/z*
$[Host\ B+peptide-4Na+6H]^{2+}$	1394.0482	1394.0505
$[Host\ B+peptide-3Na+5H]^{2+}$	1405.0445	1405.0415
$[Host\ B+peptide-4Na+7H]^{3+}$	929.7058	929.7028
$[Host\ B+peptide-3Na+6H]^{3+}$	937.0280	937.0301
$[Host\ B+peptide-2Na+5H]^{3+}$	944.3558	944.3574
$[Host\ B-4Na+4H+NH_4]^{+}$	938.1352	938.1340
$[Host\ B-3Na+4H]^{+}$	943.0851	943.0888

Equimolar Host **C** and peptide solutions were also analyzed by MS. No peaks associated with host **C**+peptide complexes were observed. However, peaks associated with non-complexed host and peptide were observed. Figure S16 shows the peaks associated with the non-complexed molecules, including $[Host\ C-2H-4Cl]^{2+}$ at *m/z* 599.3112m $[Peptide+3H]^{3+}$ at *m/z* 623.0020 and $[Peptide+2H]^{2+}$ at *m/z* 933.9983.

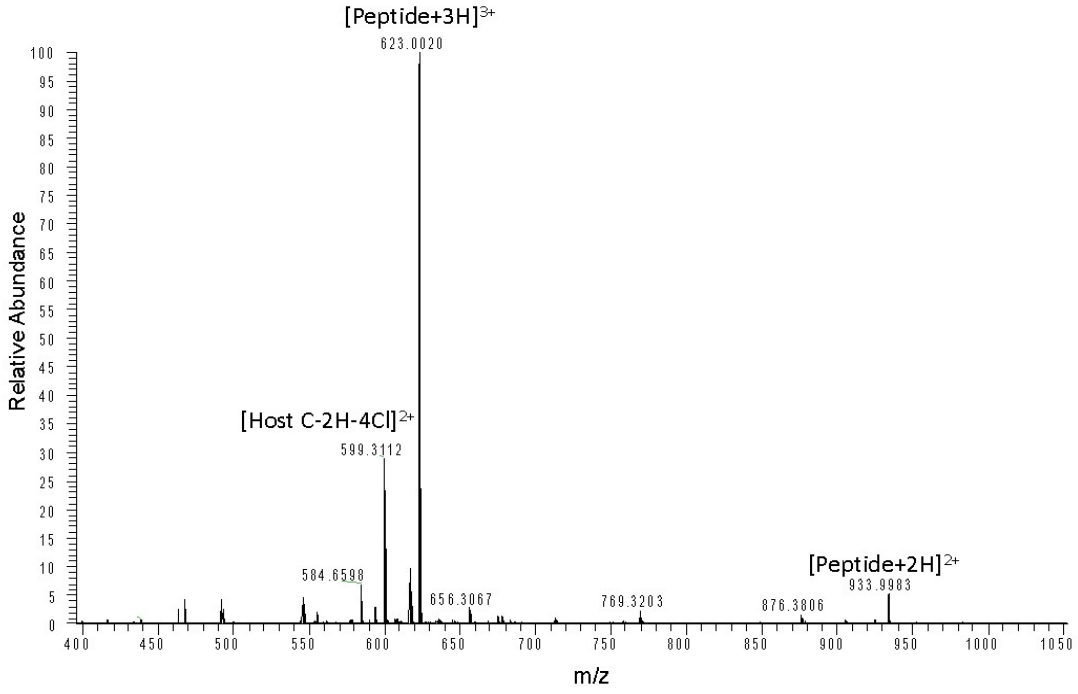

Figure S22. Positive mode ESI mass spectrum of host **C**+peptide mix after incubation for 72 hours at 37 °C. Peaks associated with the free peptide and free host are labeled.

Table S4 shows characteristic experimental and theoretical *m/z* peaks for peptide and host **C** observed in the MS of the mixture of host **C**+peptide.

Table S4. Observed and theoretical *m/z* values for mixture of host C incubated with peptide

Ion	Observed *m/z*	Theoretical *m/z*	Mass Accuracy (ppm)
Free Peptide			
$[Peptide+4H]^{4+}$	467.5033	467.504	1.497
$[Peptide+3H]^{3+}$	623.0020	623.0029	1.445
$[Peptide+2H]^{2+}$	933.9983	933.9964	2.034
Free Host C			
$[Host\ C\text{-}4HC+2HI]^{2+}$	599.3112	599.3116	0.667

VI. ^{1}H NMR Spectroscopy

For sample preparation, stock solutions of the receptor **A-C** (2 mM) and amino acids (2 mM) were prepared in D_2O. For the pure receptors and amino acid samples, 250 µL of the stock solution was transferred to an NMR tube and diluted with 250 µL of pure solvent to make a 1mM sample concentration.

For a 1:1 (**A-C**·amino acid) mixture, 250 µL of **A-C** and 250 µL of amino acid was pipetted into a clean NMR tube making 1:1 equimolar sample with 1 mM concentration of each component in the mixture.

Table S5. Summary of complexation induced chemical shift changes between amino acids and Receptors A, B and C.

Entry	Receptor A	Receptor B	Receptor C
Arginine @	+0.23, -0.13	+0.13, -0.23	-0.25
Leucine @	+0.04	+0.20, -0.23	-0.33, +0.25
Lysine @	+0.30, -0.20	0.00	-0.37
Histidine @	0.00	0.00	0.00
Isoleucine @	0.00	0.00	0.00
Phenylalanine @	0.00	0.00	0.00
Serine @	0.00	0.00	0.00
Valine @	0.00	0.00	0.00
Aspartic acid @	0.00	0.00	0.00

+ indicates largest extend of shielding (ppm) in complexation with receptor

- indicates largest extend of de-shielding (ppm) in complexation with receptor

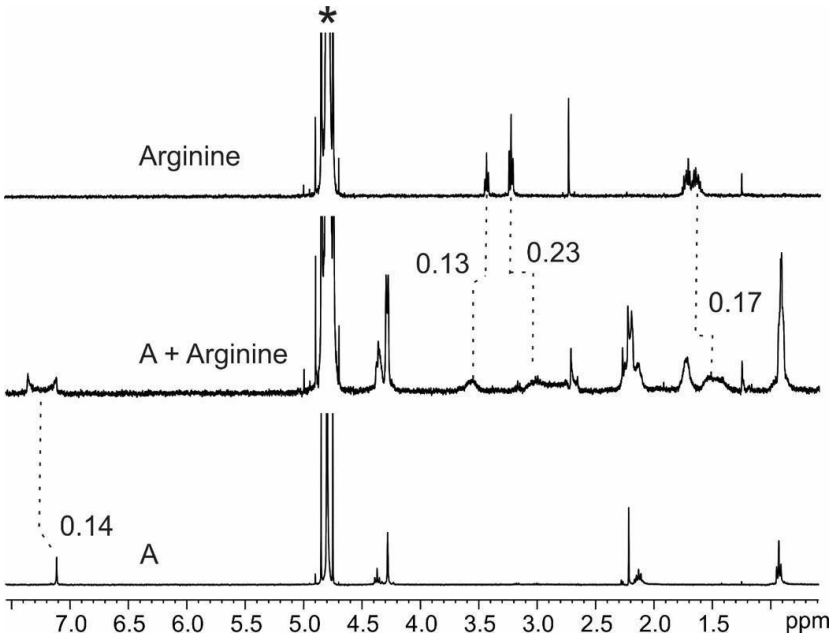

Figure S23. ^{1}H NMR spectra (D_2O, 298 K) of (a) receptor **A**, equimolar mixtures of (b) arginine@**A** and (c) arginine. The dash lines give an indication of the signal changes in ppm. Asterisks is the residual NMR solvent.

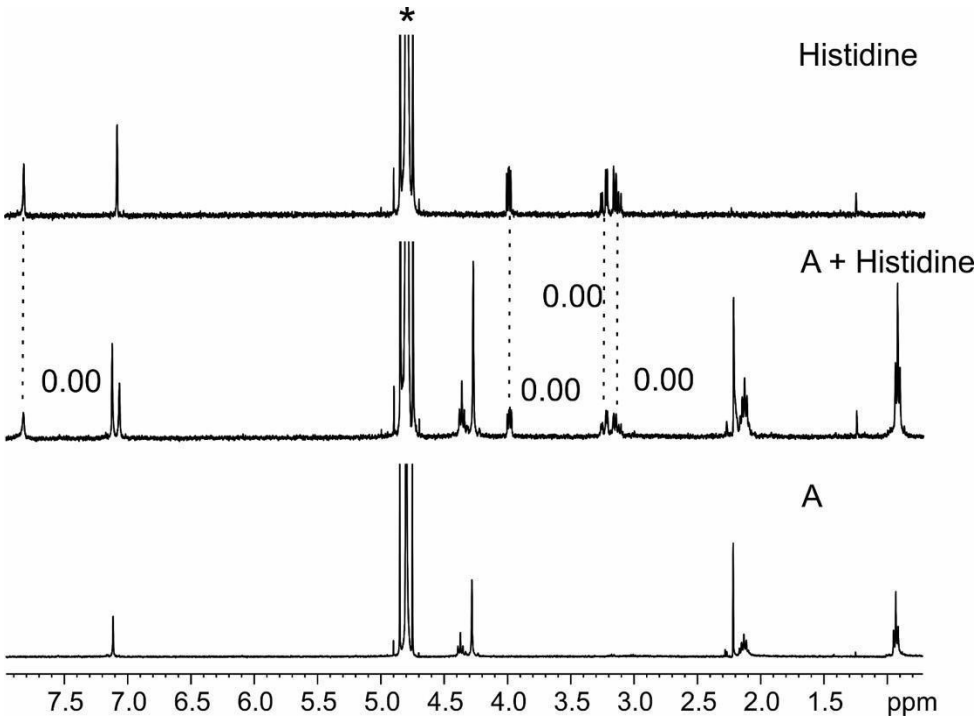

Figure S24. ^{1}H NMR spectra (D_2O, 298 K) of (a) receptor **A**, equimolar mixtures of (b) histidine@**A** and (c) histidine**.** The dash lines give an indication of the signal changes in ppm. Asterisk is the residual NMR solvent.

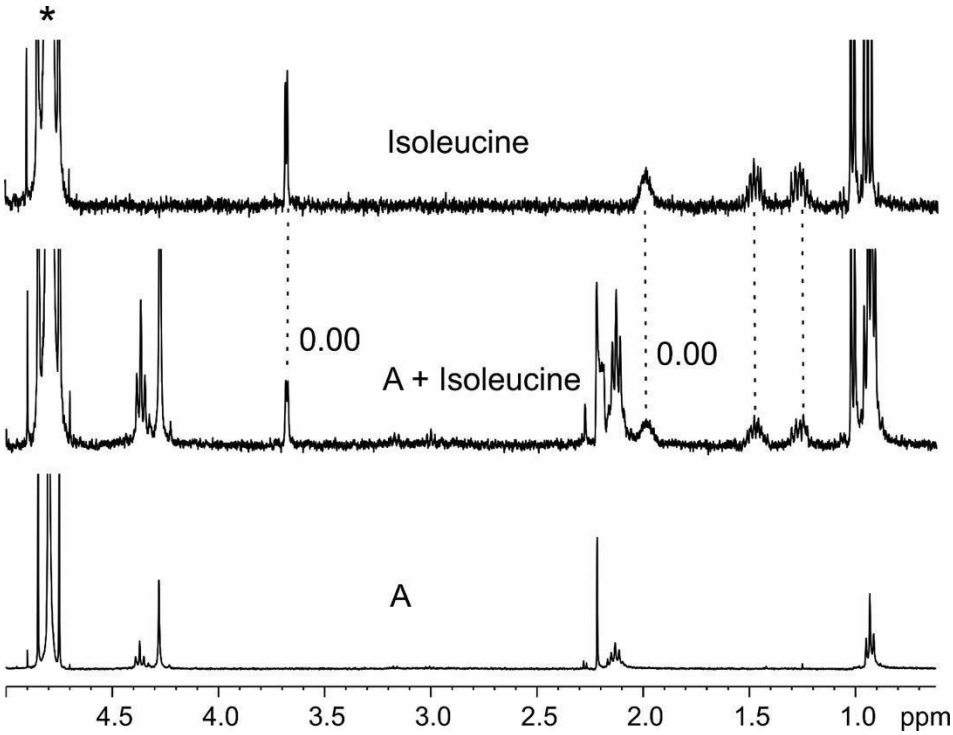

Figure S25. ^{1}H NMR spectra (D_2O, 298 K) of (a) receptor **A**, equimolar mixtures of (b) isoleucine@**A** and (c) Isoleucine. The dash lines give an indication of the signal changes in ppm. Asterisk is the residual NMR solvent.

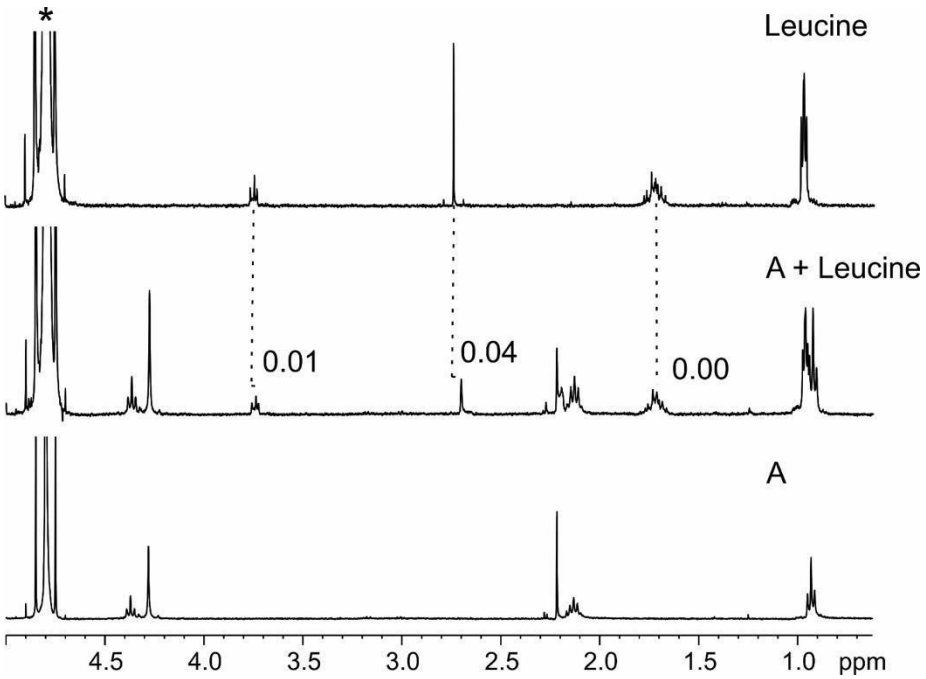

Figure S26. ^{1}H NMR spectra (D_2O, 298 K) of (a) receptor **A**, equimolar mixtures of (b) leucine@**A** and (c) leucine. The dash lines give an indication of the signal changes in ppm. Asterisk is the residual NMR solvent.

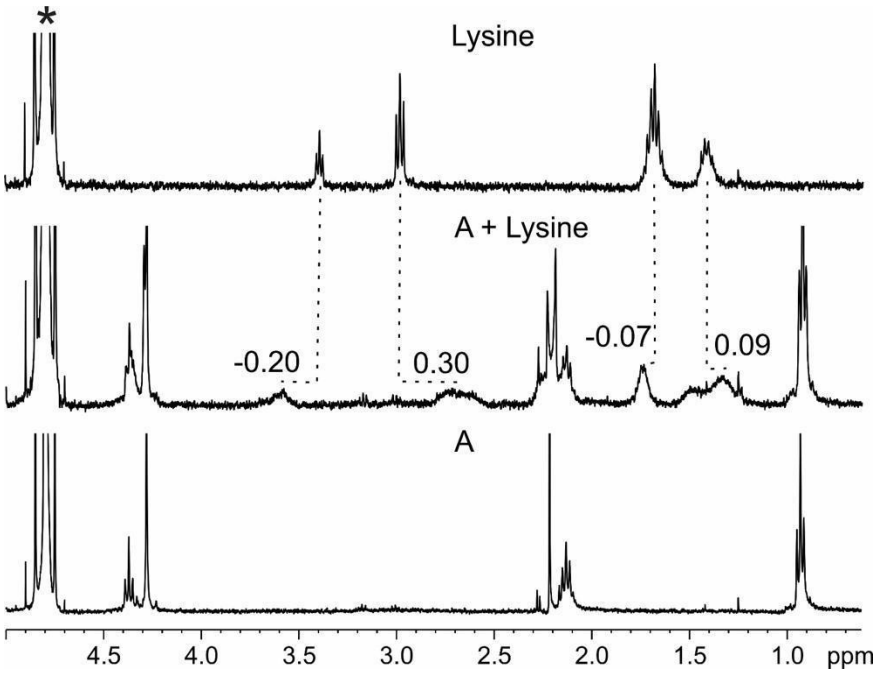

Figure S27. ^{1}H NMR spectra (D_2O, 298 K) of (a) receptor **A**, equimolar mixtures of (b) lysine@**A** and (c) lysine. The dash lines give an indication of the signal changes in ppm. Asterisk is the residual NMR solvent.

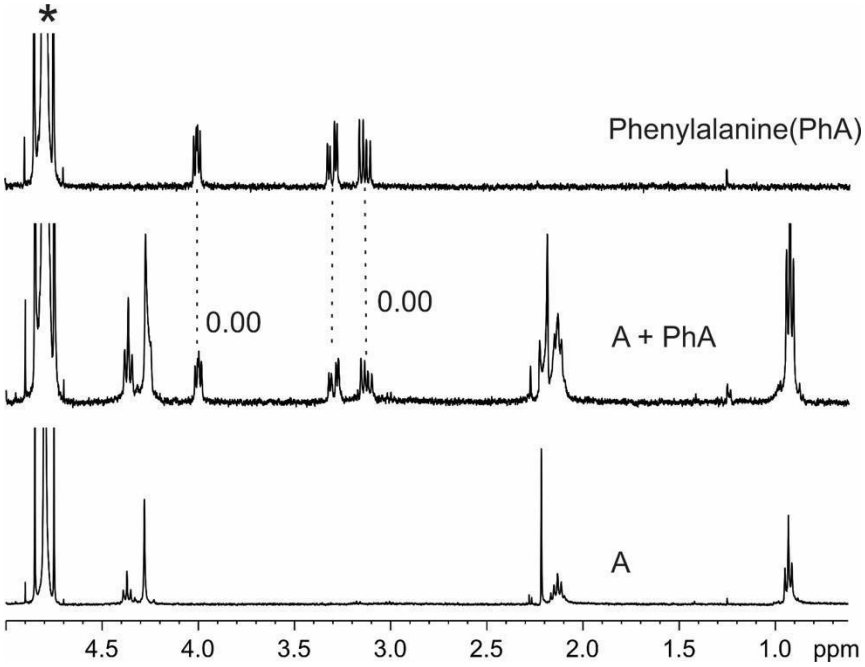

Figure S28. ^{1}H NMR spectra (D_2O, 298 K) of (a) receptor **A**, equimolar mixtures of (b) phenylalanine@**A** and (c) phenylalanine. The dash lines give an indication of the signal changes in ppm. Asterisk is the residual NMR solvent.

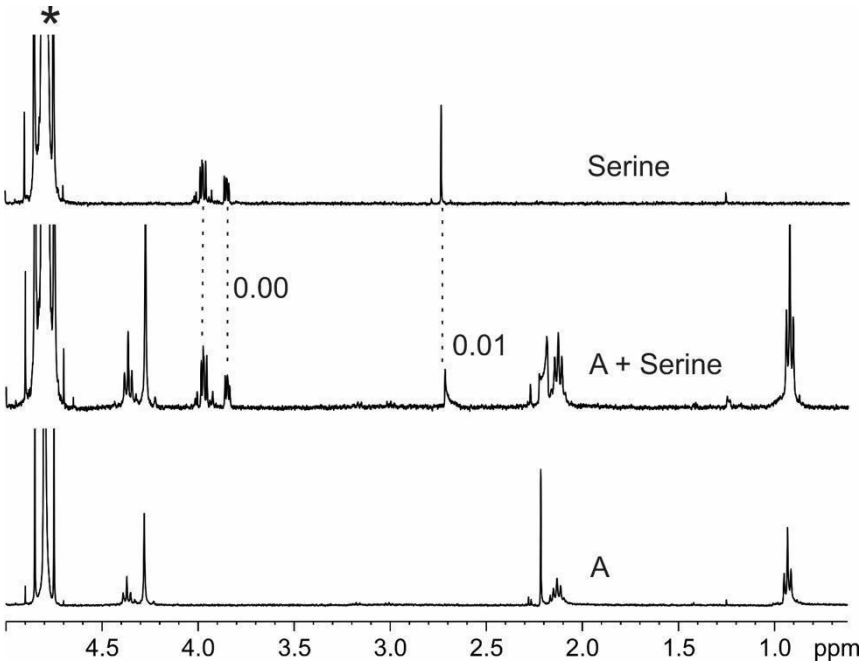

Figure S29. ^{1}H NMR spectra (D_2O, 298 K) of (a) receptor **A**, equimolar mixtures of (b) serine@**A** and (c) serine. The dash lines give an indication of the signal changes in ppm. Asterisk is the residual NMR solvent.

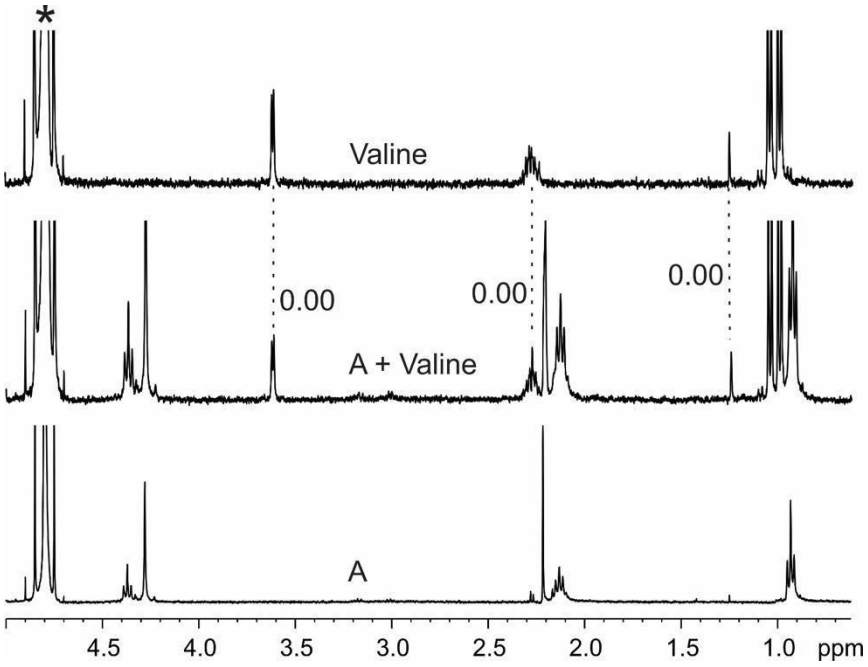

Figure S30. ^{1}H NMR spectra (D_2O, 298 K) of (a) receptor **A**, equimolar mixtures of (b) valine@**A** and (c) valine. The dash lines give an indication of the signal changes in ppm. Asterisk is the residual NMR solvent.

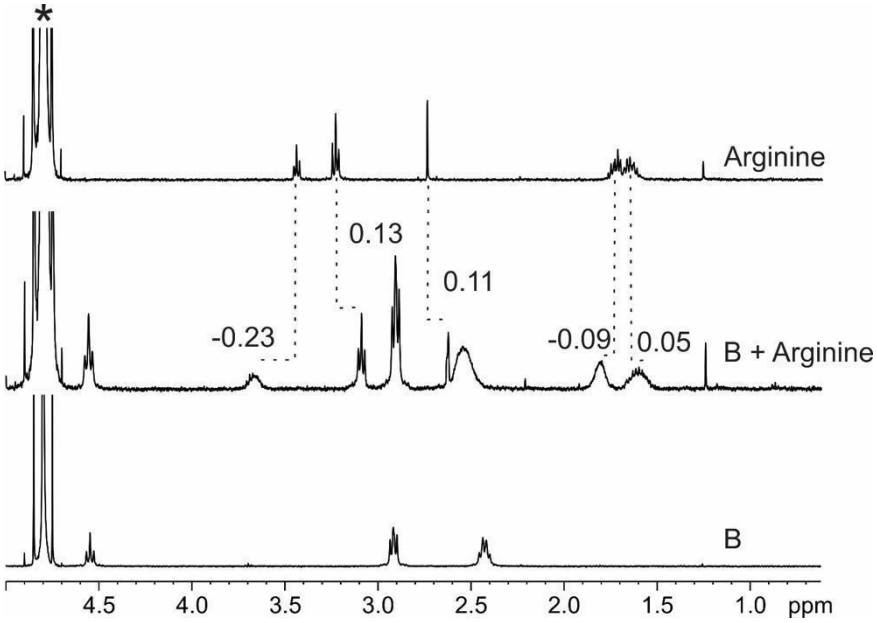

Figure S31. ^{1}H NMR spectra (D_2O, 298 K) of (a) receptor **B**, equimolar mixtures of (b) arginine@**B** and (c) arginine. The dash lines give an indication of the signal changes in ppm. Asterisk is the residual NMR solvent.

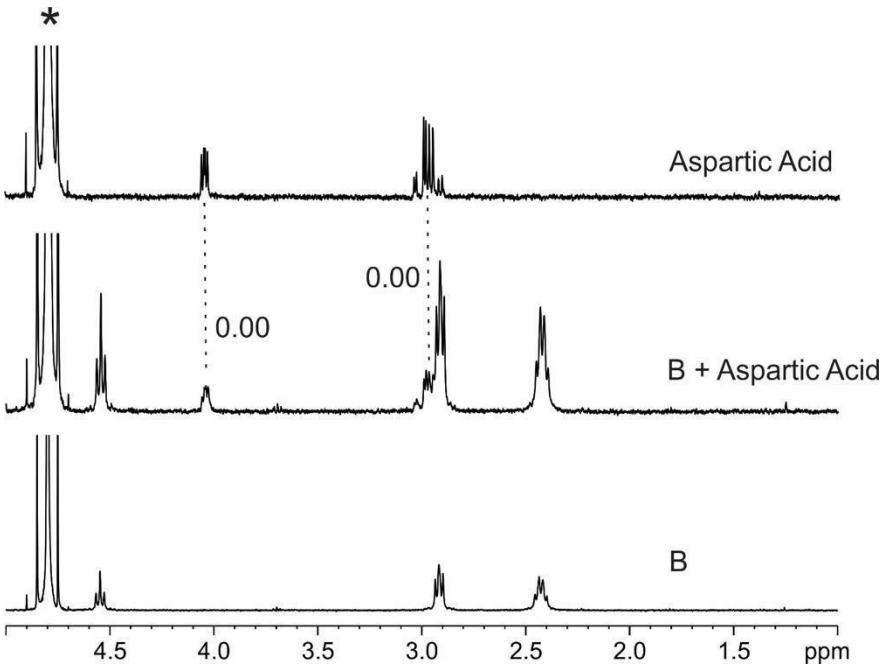

Figure S32. ^{1}H NMR spectra (D_2O, 298 K) of (a) receptor **B**, equimolar mixtures of (b) aspartic acid@**B** and (c) aspartic acid. The dash lines give an indication of the signal changes in ppm. Asterisk is the residual NMR solvent.

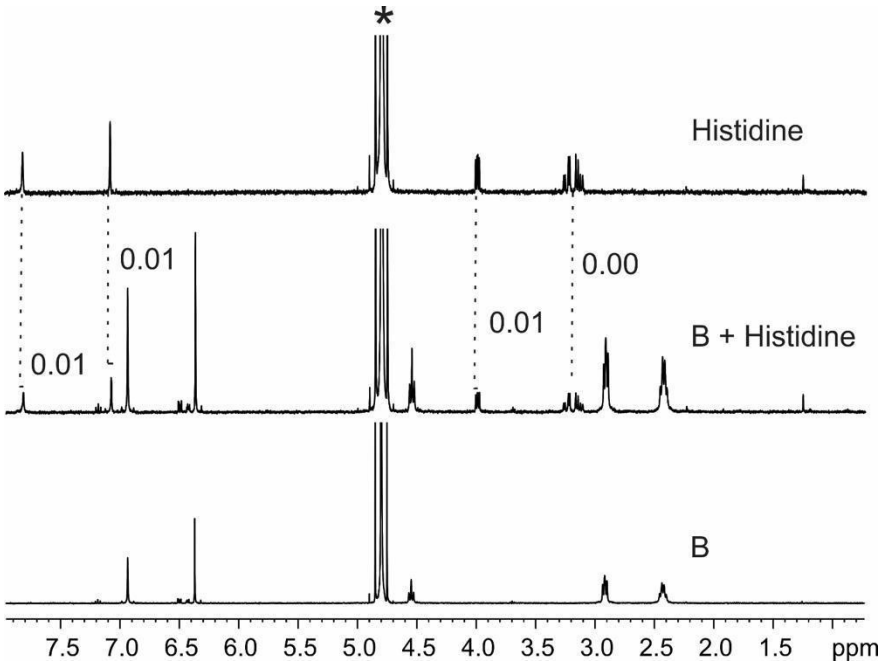

Figure S33. ^{1}H NMR spectra (D_2O, 298 K) of (a) receptor **B**, equimolar mixtures of (b) histidine@**B** and (c) histidine. The dash lines give an indication of the signal changes in ppm. Asterisk is the residual NMR solvent.

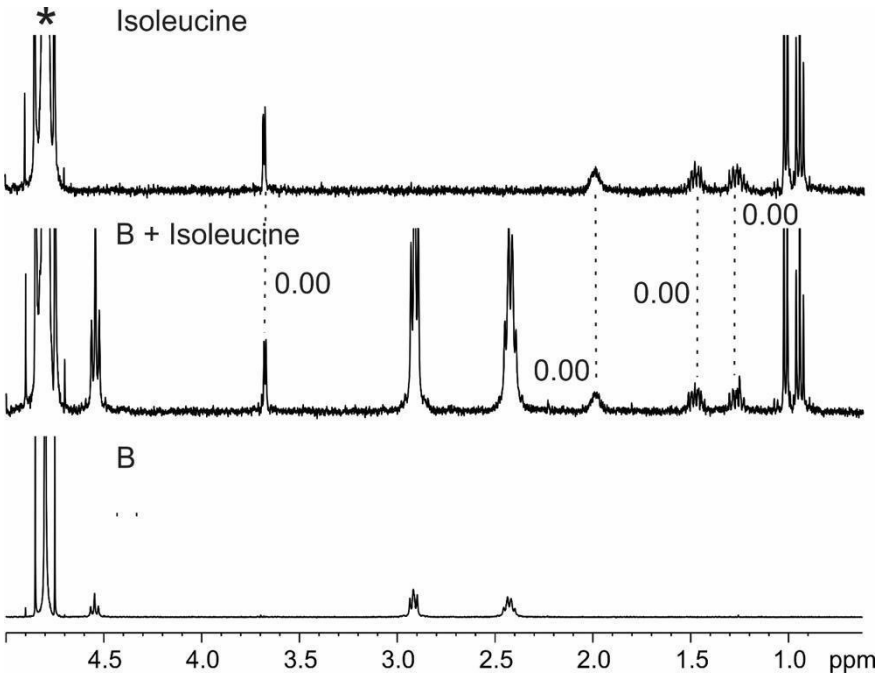

Figure S34. ^{1}H NMR spectra (D_2O, 298 K) of (a) receptor **B**, equimolar mixtures of (b) isoleucine@**B** and (c) isoleucine. The dash lines give an indication of the signal changes in ppm. Asterisk is the residual NMR solvent.

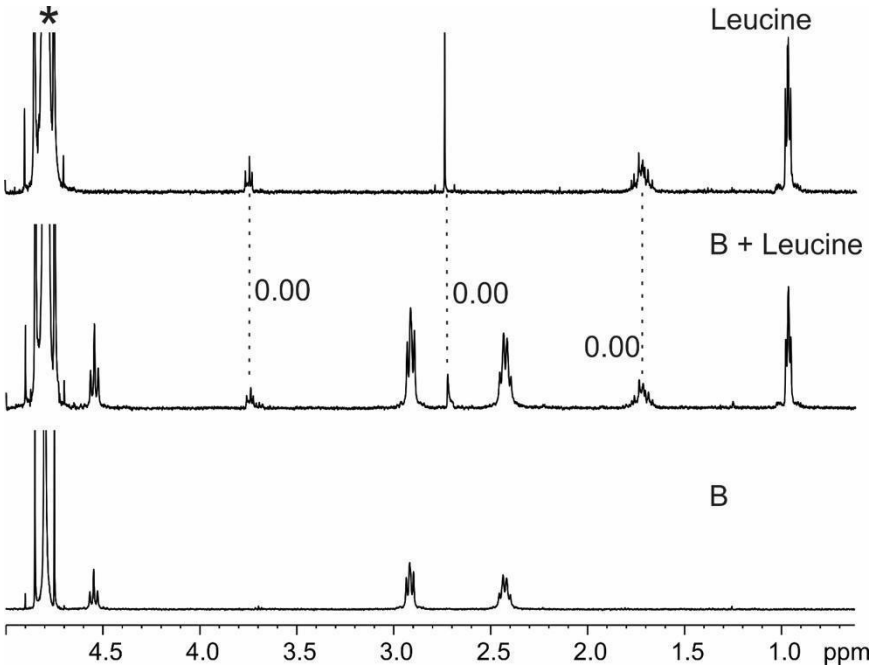

Figure S35. ^{1}H NMR spectra (D_2O, 298 K) of (a) receptor **B**, equimolar mixtures of (b) leucine@**B** and (c) leucine. The dash lines give an indication of the signal changes in ppm. Asterisk is the residual NMR solvent.

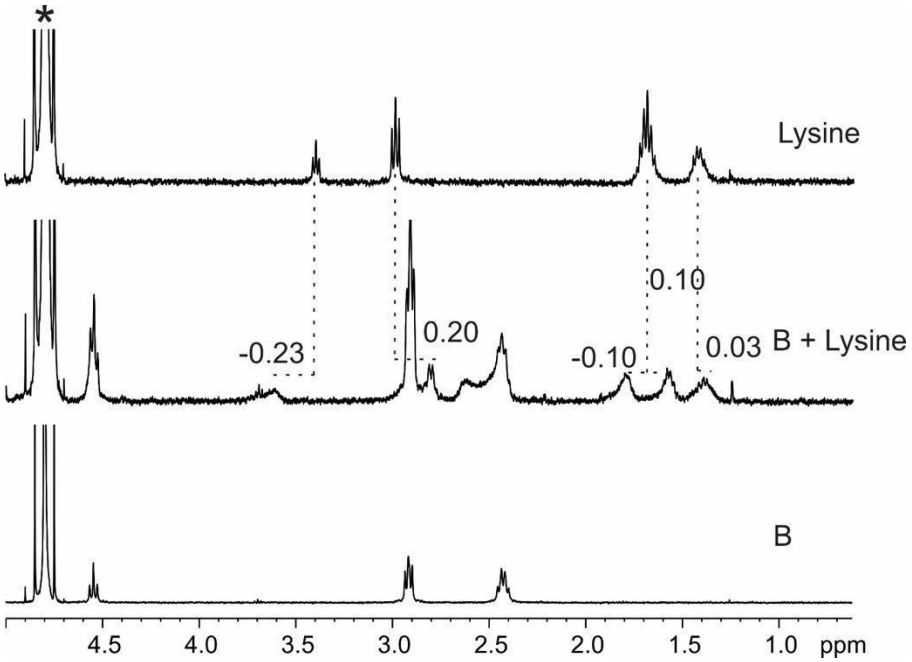

Figure S36. ^{1}H NMR spectra (D_2O, 298 K) of (a) receptor **B**, equimolar mixtures of (b) lysine@**B** and (c) lysine. The dash lines give an indication of the signal changes in ppm. Asterisk is the residual NMR solvent.

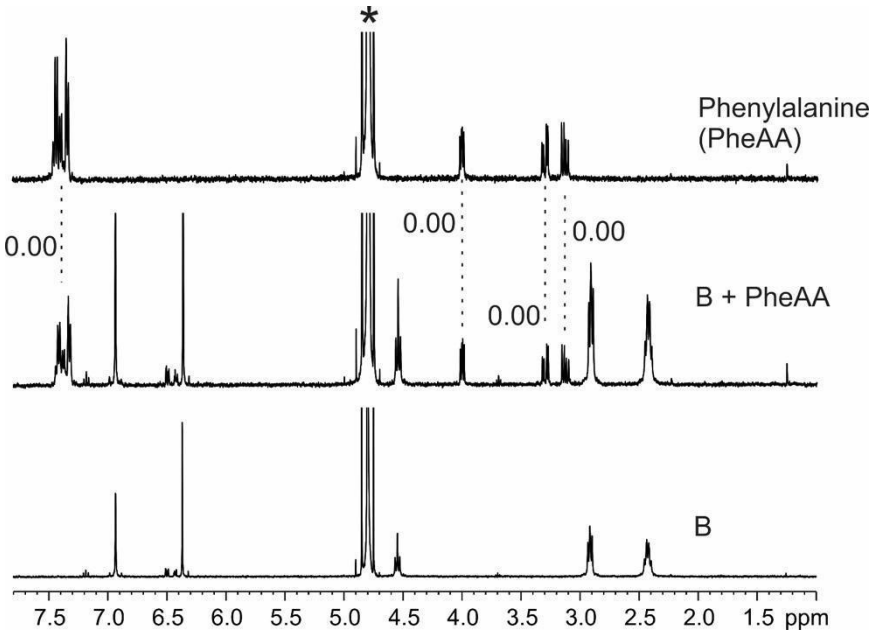

Figure S37. ^{1}H NMR spectra (D_2O, 298 K) of (a) receptor **B**, equimolar mixtures of (b) phenylalanine@**B** and (c) phenylalanine. The dash lines give an indication of the signal changes in ppm. Asterisk is the residual NMR solvent.

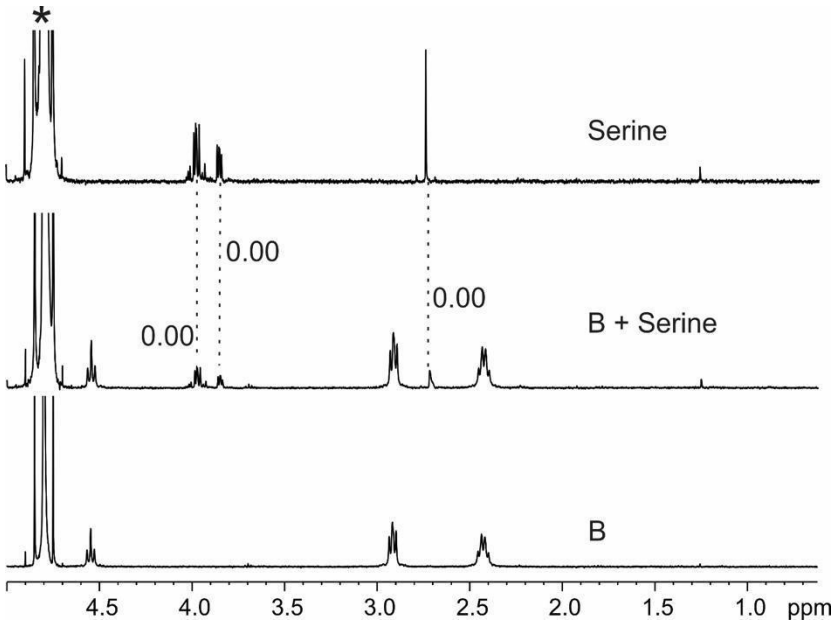

Figure S38. ^{1}H NMR spectra (D_2O, 298 K) of (a) receptor **B**, equimolar mixtures of (b) serine@**B** and (c) serine. The dash lines give an indication of the signal changes in ppm. Asterisk is the residual NMR solvent.

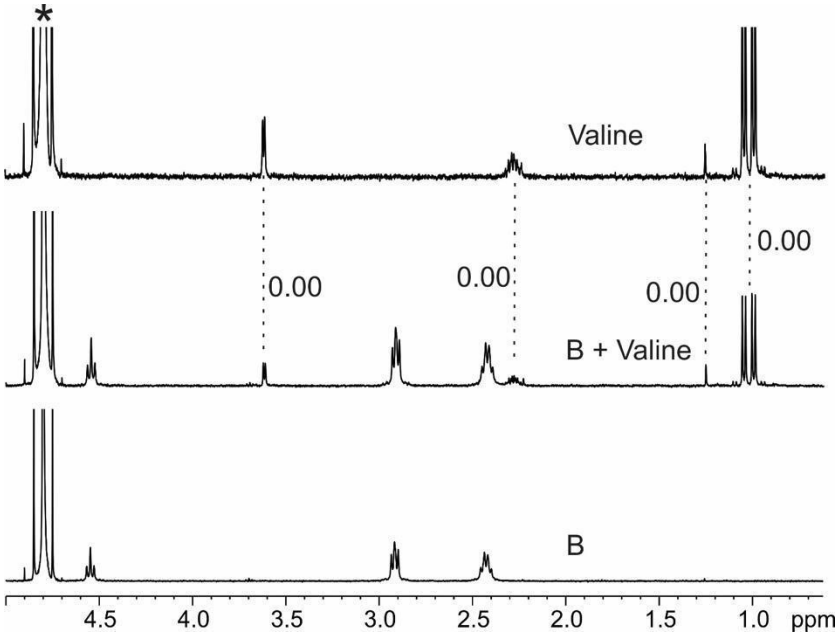

Figure S39. ^{1}H NMR spectra (D_2O, 298 K) of (a) receptor **B**, equimolar mixtures of (b) valine@**B** and (c) valine. The dash lines give an indication of the signal changes in ppm. Asterisk is the residual NMR solvent.

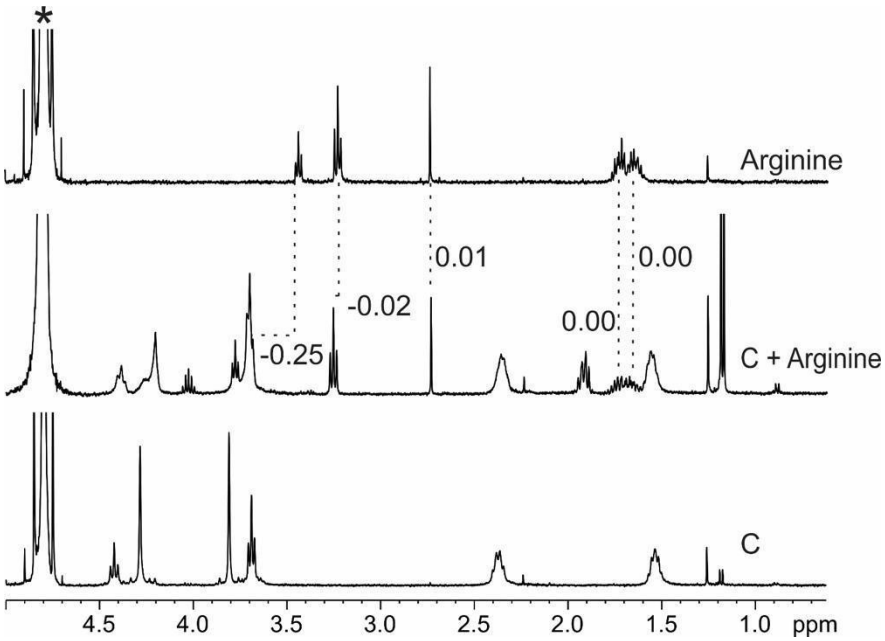

Figure S40. ^{1}H NMR spectra (D_2O, 298 K) of (a) receptor **C**, equimolar mixtures of (b) arginine@**C** and (c) arginine. The dash lines give an indication of the signal changes in ppm. Asterisk is the residual NMR solvent.

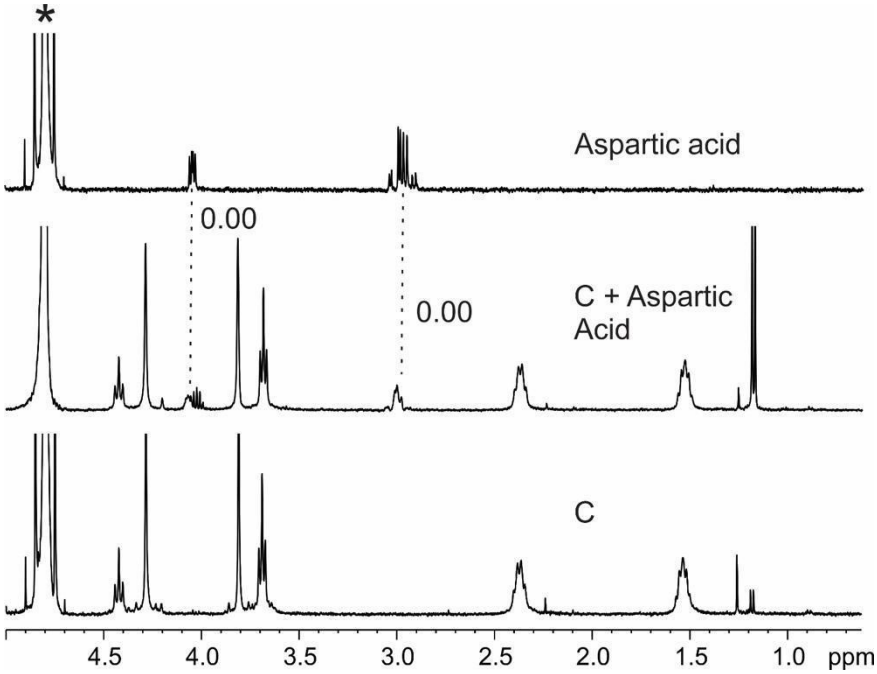

Figure S41. ^{1}H NMR spectra (D_2O, 298 K) of (a) receptor **C**, equimolar mixtures of (b) aspartic acid@**C** and (c) aspartic acid. The dash lines give an indication of the signal changes in ppm. Asterisk is the residual NMR solvent.

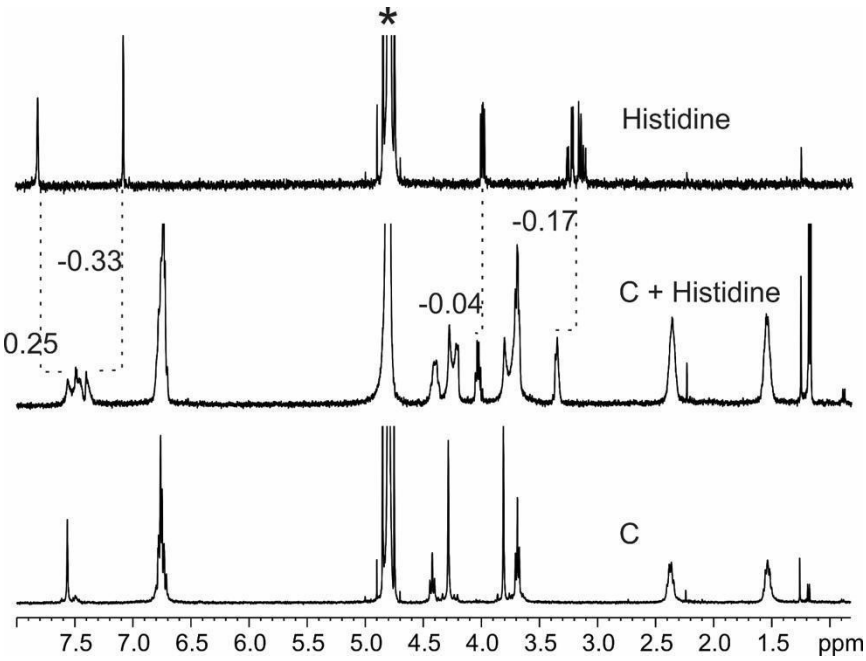

Figure S42. ^{1}H NMR spectra (D_2O, 298 K) of (a) receptor **C**, equimolar mixtures of (b) histidine@**C** and (c) histidine. The dash lines give an indication of the signal changes in ppm. Asterisk is the residual NMR solvent.

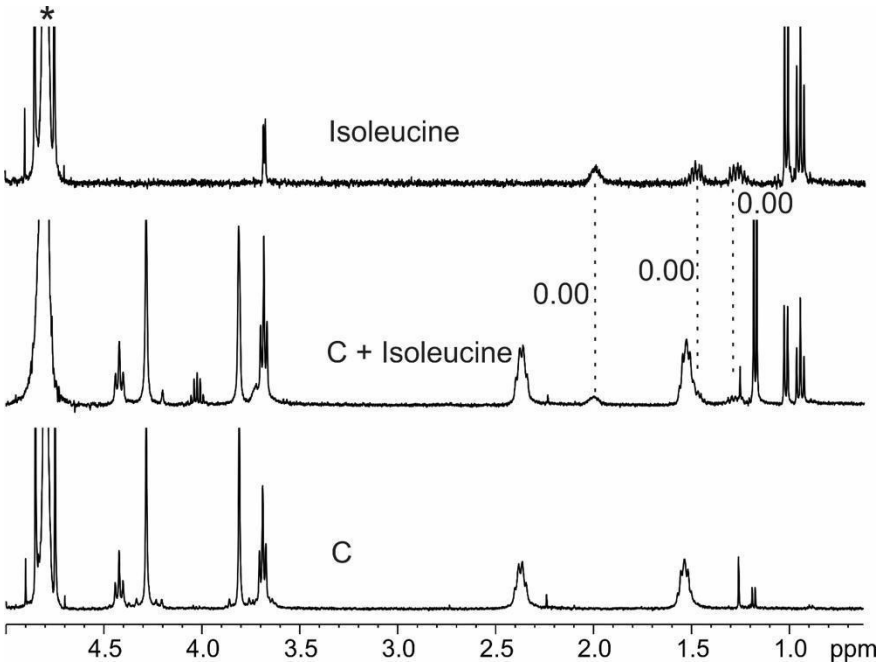

Figure S43. ^{1}H NMR spectra (D_2O, 298 K) of (a) receptor **C**, equimolar mixtures of (b) isoleucine@**C** and (c) isoleucine. The dash lines give an indication of the signal changes in ppm. Asterisk is the residual NMR solvent.

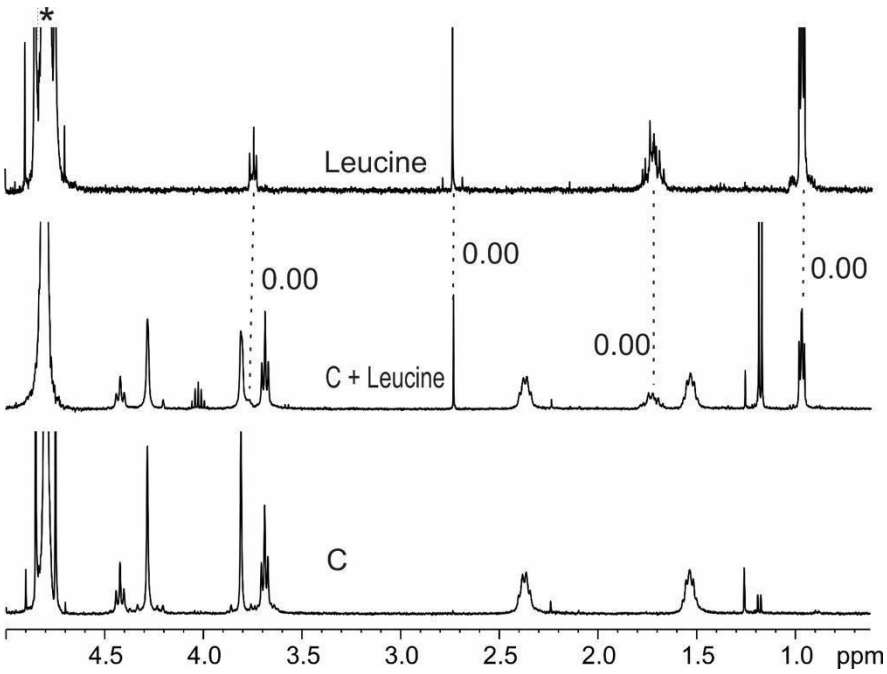

Figure S44. ^{1}H NMR spectra (D_2O, 298 K) of (a) receptor **C**, equimolar mixtures of (b) leucine@**C** and (c) leucine. The dash lines give an indication of the signal changes in ppm. Asterisk is the residual NMR solvent.

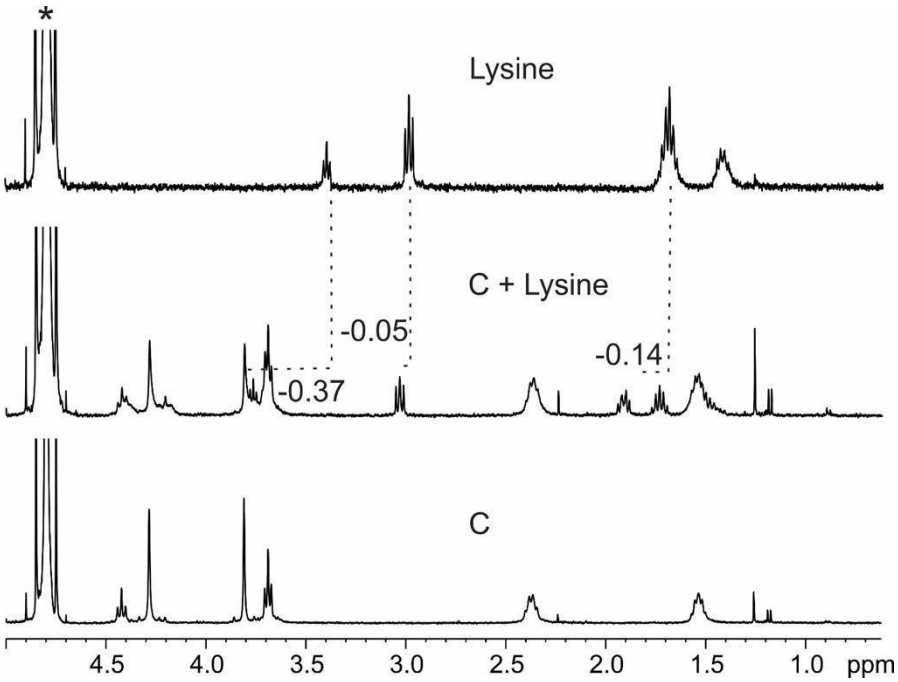

Figure S45. ^{1}H NMR spectra (D_2O, 298 K) of (a) receptor **C**, equimolar mixtures of (b) lysine@**C** and (c) lysine. The dash lines give an indication of the signal changes in ppm. Asterisk is the residual NMR solvent.

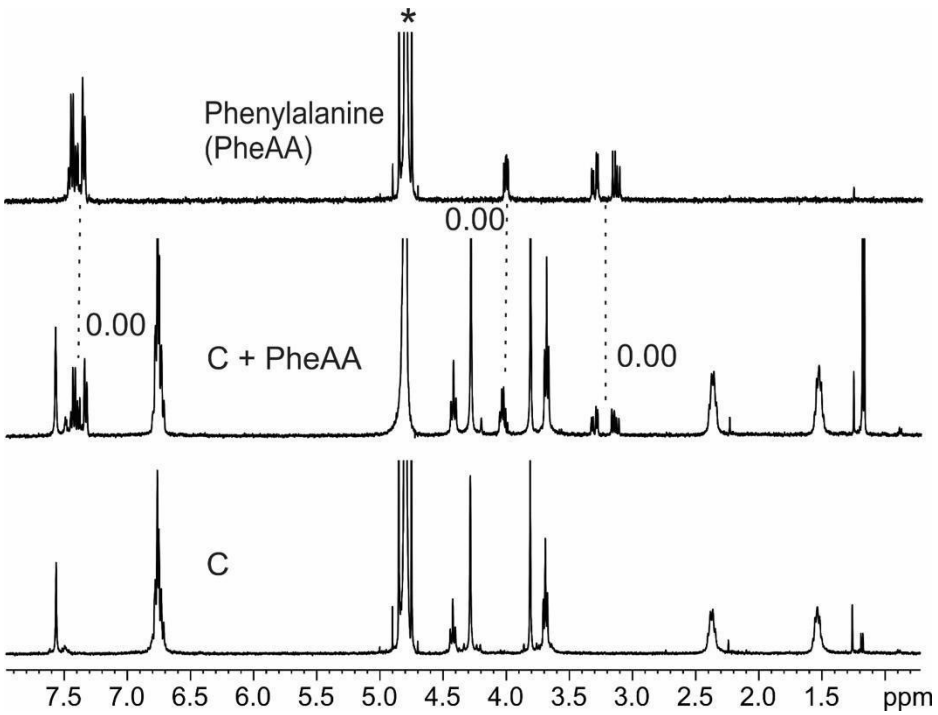

Figure S46. ^{1}H NMR spectra (D_2O, 298 K) of (a) receptor **C**, equimolar mixtures of (b) phenylalanine@**C** and (c) phenylalanine. The dash lines give an indication of the signal changes in ppm. Asterisk is the residual NMR solvent.

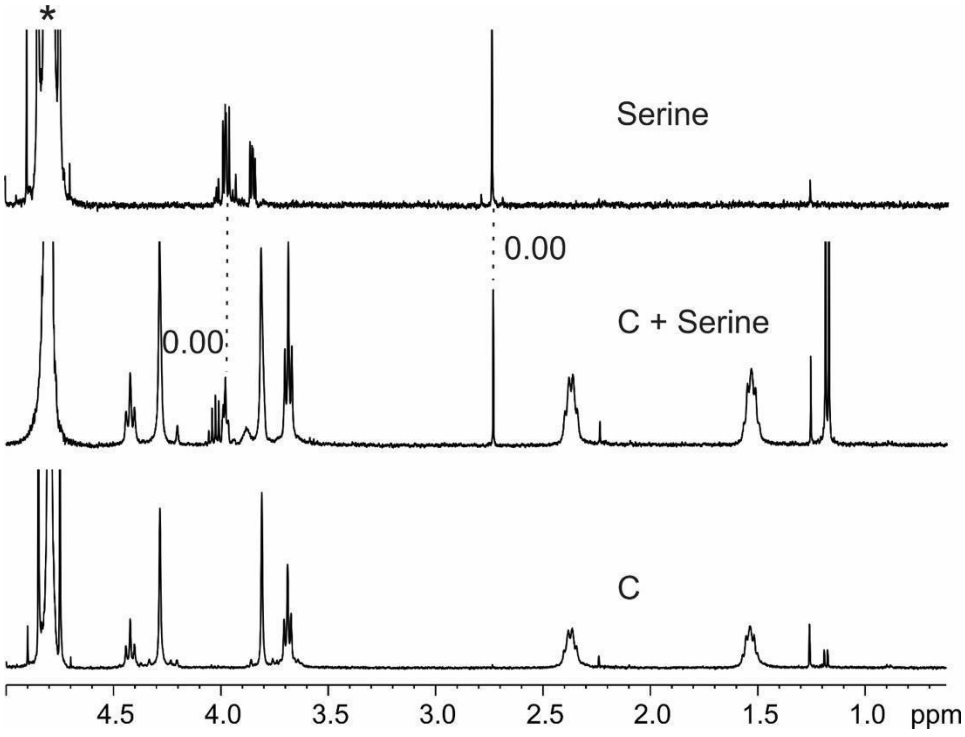

Figure S47. ^{1}H NMR spectra (D_2O, 298 K) of (a) **C**, equimolar mixtures of (b) serine@**C** and (c) serine. The dash lines give an indication of the signal changes in ppm. Asterisk is the residual NMR solvent.

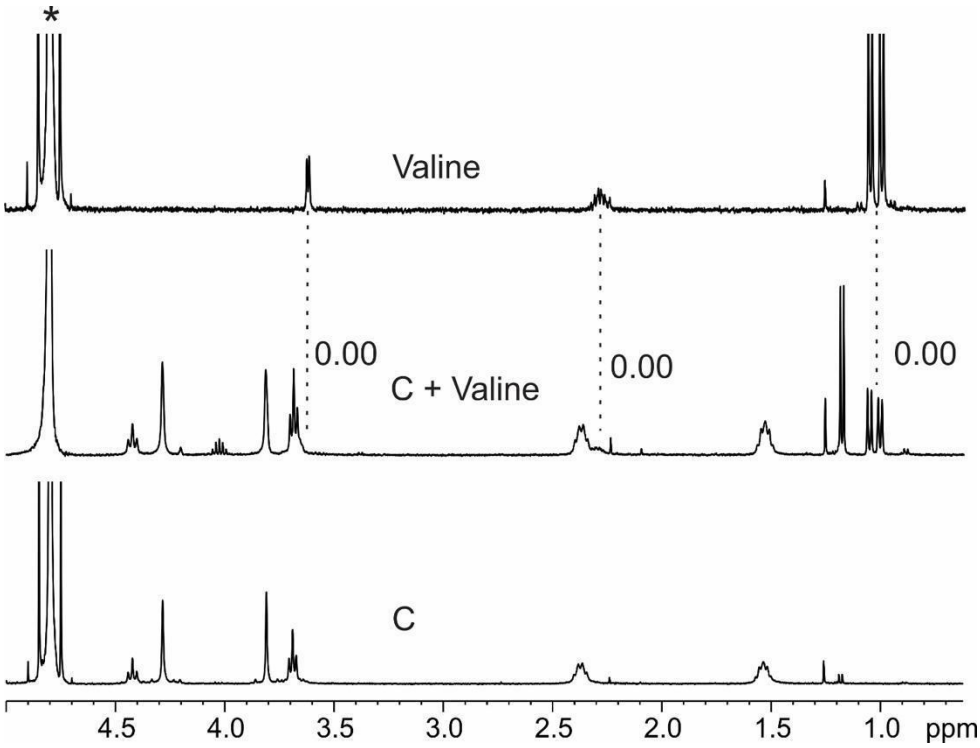

Figure S48. ^{1}H NMR spectra (D_2O, 298 K) of (a) receptor **C**, equimolar mixtures of (b) valine@**C** and (c) valine. The dash lines give an indication of the signal changes in ppm. Asterisk is the residual NMR solvent.

VII. Isothermal Titration Calorimetry (ITC)

VP-ITC instrument made by MicroCal was used to determine the molar enthalpy (ΔH) of complexation. Subsequent fitting of the data to a 1:1 binding model using Origin software provides binding constant (K), change in enthalpy (ΔH) and change in entropy (ΔS). The data were fitted to a one-site binding model. The ITC experiment was carried out by filling the sample cell with one sample (1 mM), filling the syringe with the titrant (15 mM), and titrating via a computer-automated injector at 298 K. Blank titrations into plain solvent were also performed and subtracted from the corresponding titration to remove any effect from the heats of dilution from the titrant.

Table S6. Interaction parameters between receptors **A**, **B** and **C** and selected amino acids in Tris buffer. All the data shown were fitted to one set of sites binding model at 298K.

Complex	K_a *(× 10³) M⁻¹*	*ΔH° kcal/mol*	*TΔS° kcal/mol*	*ΔG° kcal/mol*
A•				
Arginine	7.27±1.28	-15.70±3.85	-10.43	-5.27
Lysine	5.89± 0.88	-12.07±2.04	-6.45	-5.62
Histidine	2.94±0.39	-2.59±0.16	6.91	-9.50
B•				
Arginine	1.42±0.73	-0.60±0.26	3.70	-4.30
Lysine	-	-	-	-
Histidine	-	-	-	-
C•				
Arginine	1.66±0.13	-1.07±0.05	3.31	-4.38
Lysine	0.78±0.12	-1.40±0.14	2.55	-3.95
Histidine	-	-	-	-
Aspartic Acid	-	-	-	-

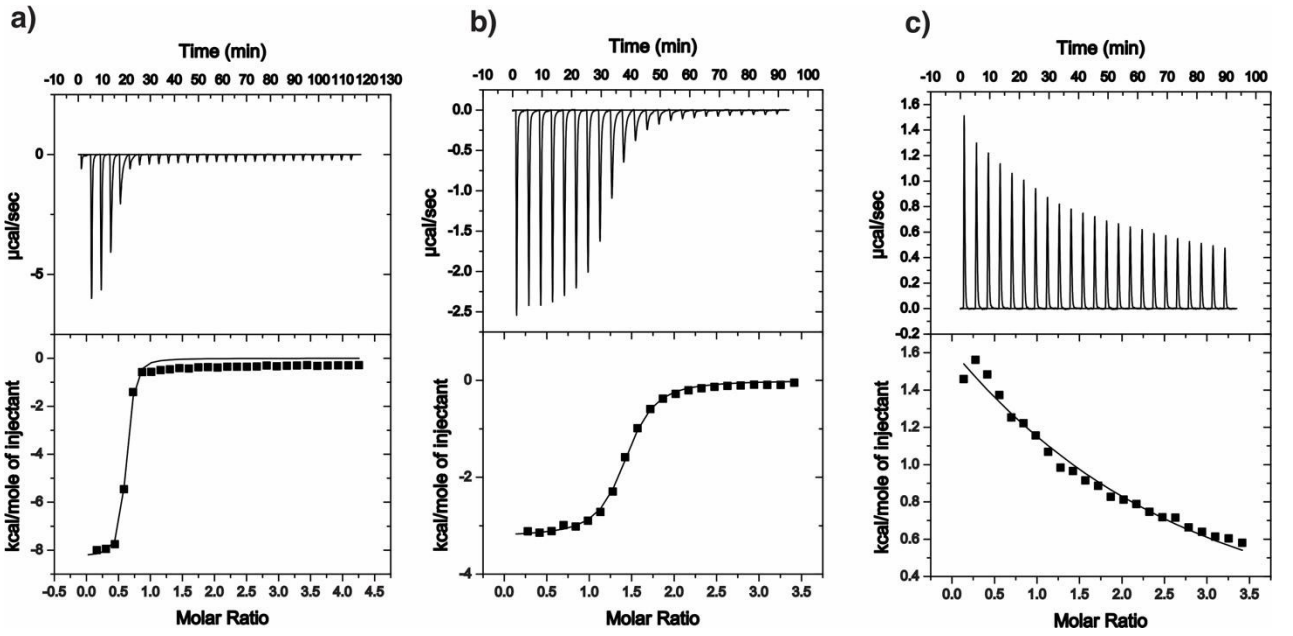

Figure S49. ITC traces of the titration of crystallin peptide with receptors **A**, **B** and **C** (a, b and c respectively) at 298 K in water. All the data were fitted to a one-site binding model.

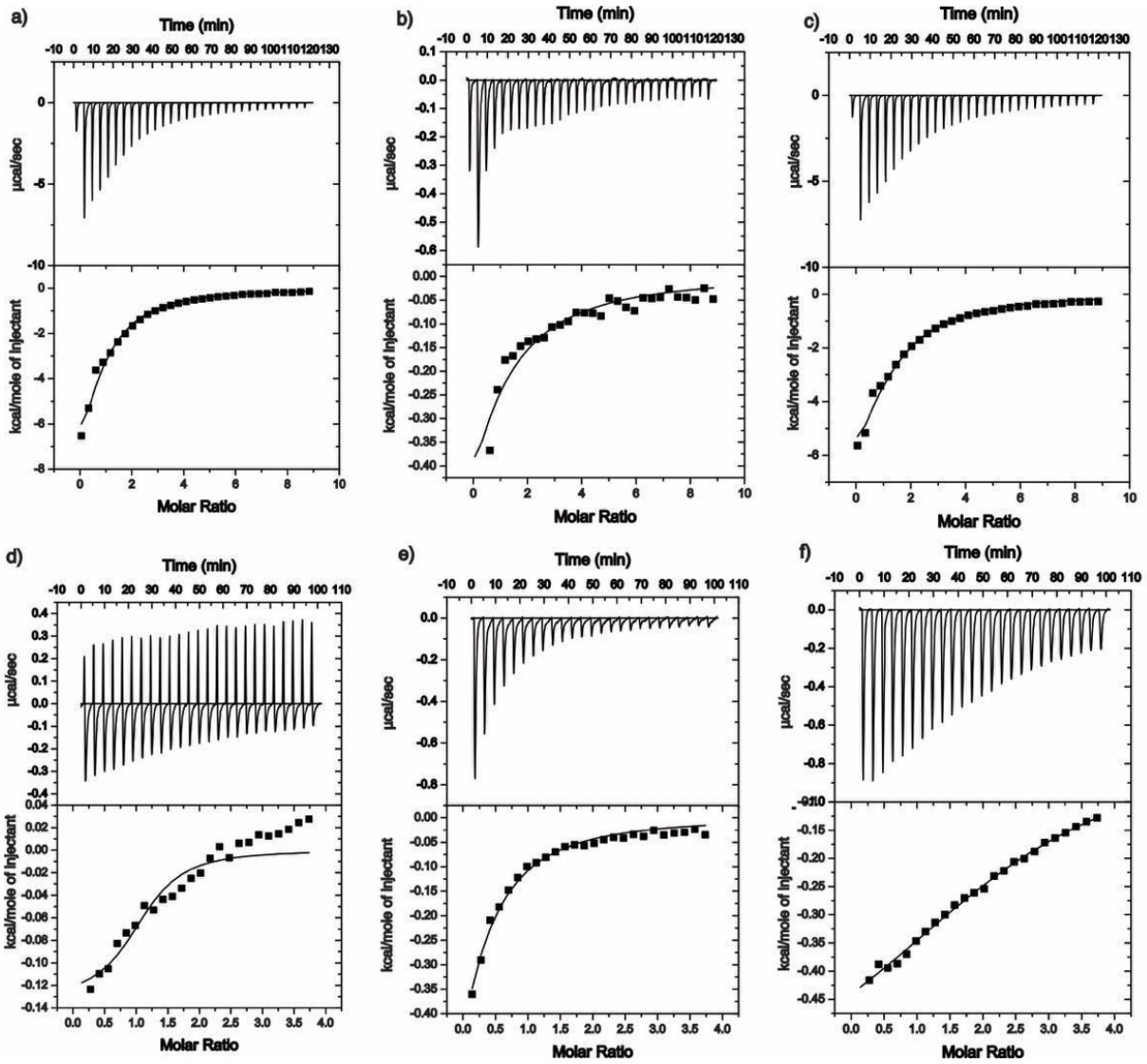

Figure S50. ITC traces of the titration of receptor **A** with amino acids at 298 K. The data was fitted to a one-site binding model for (a) arginine@**A**, (b) histidine@**A,** and (c) lysine@**A** in water. (d) arginine@**A**, (e) histidine@**A,** and lysine@**A** were in 10mM tris buffer at pH 7.4.

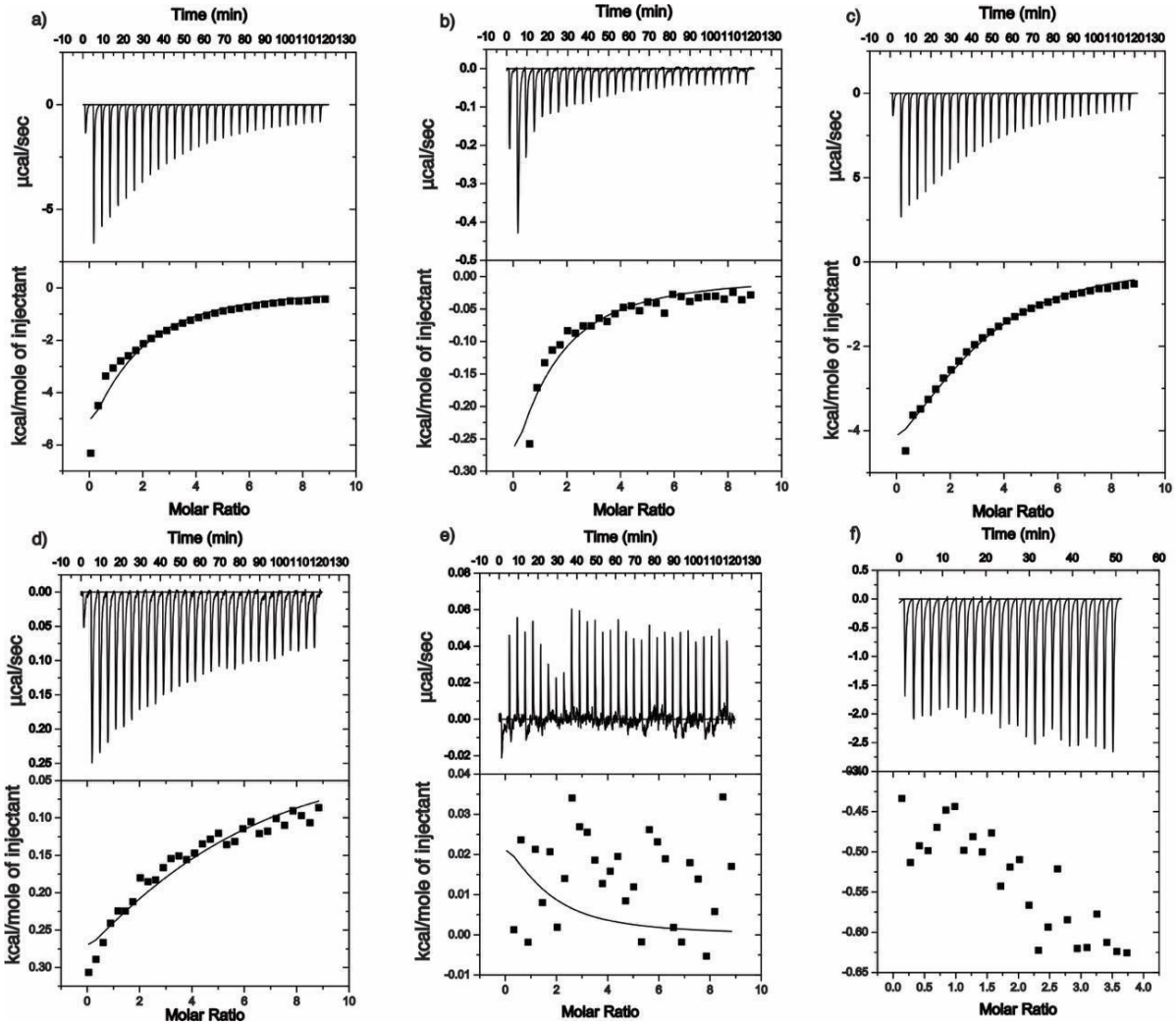

Figure S51. ITC traces of the titration of receptor **B** with amino acids at 298 K. The data was fitted to a one site binding model for (a) arginine@**B**, (b) histidine@**B** and (c) lysine@**B** in water and (d) arginine@**B** in 10mM tris buffer (ph 7.4). (e) histidine@**B** and (f) lysine@**B** does not bind.

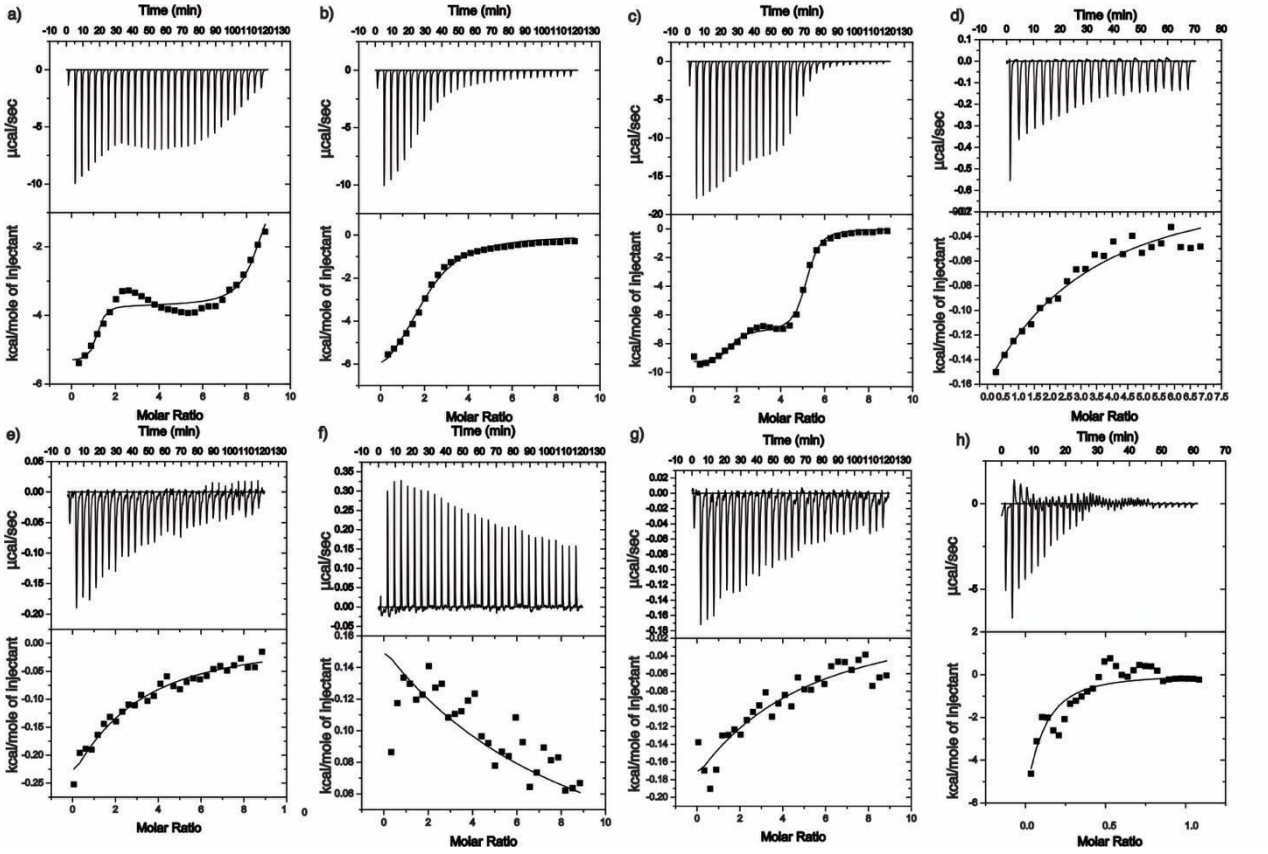

Figure S52. ITC traces of the titration of receptor **C** with amino acids at 298 K. The data were fitted to a one-site binding model for (b) histidine@**C** and (d) aspartic acid@**C** in water. (e) arginine@**C**, (g) lysine@**C** were fitted to one-site binding model in 10mM tris buffer at pH 7.4 and (a) arginine@**C**, (c) lysine@**C**, (f) histidine@**C** and (h) asparticacid@**C** could not be fitted without large errors.

VIII. Computation

Structure Preparation and Docking

Alpha-crystallin A protein (pdb ID:6t1r) was obtained from the pdb website.[4] The protein preparation involved removing extraneous chains, ions, alternate conformations, and solvent molecules using UCSF Chimera dock prep module.[5] Missing hydrogen atoms were added, histidine and aspartic acid residues were visually adjusted for correct protonation states. The protein was capped and minimized to correct the unfavorable interactions and atom clashes. The structures were saved according to dock6 manual for protein preparation[ref]. The chain A:SER75-PHE80 peptide sequence ready for the next steps.

The 3D host structure models were constructed and minimized using Gaussian 09 suite of quantum chemistry programs at b3lyp/6-31g(d,p) in cpcm water.[6] Charges were added to the hosts using Add Charge tool and selecting AM1-BCC charge method in Chimera and then saved.

Molecular Docking was performed using the dock6 [ref] program in default configuration, first, holding both host and peptide rigid, ranking the scores and redocking the top three hits in place with the host molecule flexible. The topmost ranked pose for each host was picked. The docking scores were reported, and the docked poses were prepared for molecular dynamics simulation.

Molecular Dynamics

The molecular dynamics (MD) system preparation was done in the Maestro GUI and simulations were done using desmond from DE Shaw Research.[7] A cubic box with 10Å buffer around the TIP3P solvated complex was selected. A 150mM NaCl solute concentration was added to the matrix. Sodium ions were then added to neutralize the corresponding total charge on the complex. OPLS2005 forcefield was used. The system was then minimized in desmond.

The relaxation and equilibration followed the standard desmond protocol. Production MD was carried out for 100 ns in the NPT ensemble at 300 K without any particle restraint. A Nose-hoover chain with thermostat relaxation time of 1 ps was used. In addition, a barostat of Martyna-Tobias-Klein method with 2 ps relaxation time and an isotropic coupling style was employed. A multiple time step RESPA integrator with 2 fs for near and 6 fs for far sampling was chosen. A smooth particle mesh Ewald with cutoff at 9.0 Å and an Ewald tolerance of $1x10^{-9}$ was used. Energy and time evolution recording was done every 1.2 ps and 100 ps respectively. The binding energy for the MD trajectory calculations were then carried using MMGBSA method.[8]

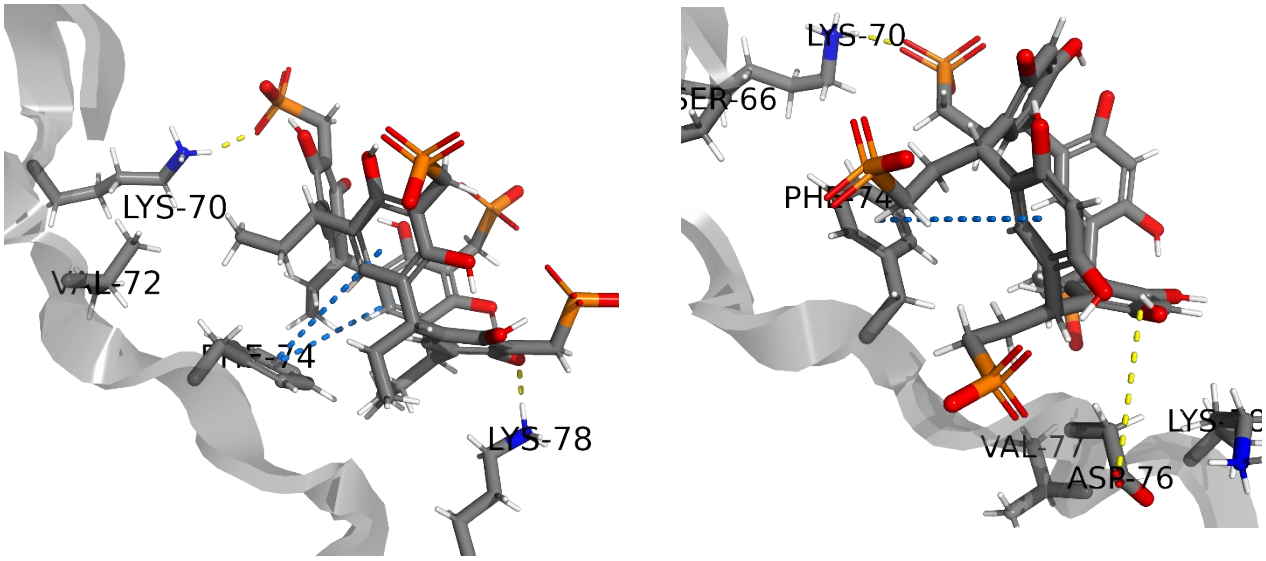

Figure S53. Zoomed-in images of the interaction between peptide•**A** (left) and peptide•**B** (right) binding. Different types of interactions are shown using dotted lines of different colors: hydrogen bonding (yellow), pi-stacking (blue). The interaction between the peptide and host **A** is stable from 7.6 ns to the rest of the simulation time of 100 ns whereas the peptide and host **B** is stable for the whole simulation time of 100 ns.

IX. References

(1) Kazakova, E. K.; Makarova, N. A.; Ziganshina, A. U.; Muslinkina, L. A.; Muslinkin, A. A.; Habicher, W. D. Novel Water-Soluble Tetrasulfonatomethylcalix[4]Resorcinarenes. *Tetrahedron Lett.* **2000**, *41* (51), 10111–10115. https://doi.org/10.1016/S0040-4039(00)01798-6.

(2) Twum, K.; Rautiainen, J. M.; Yu, S.; Truong, K. N.; Feder, J.; Rissanen, K.; Puttreddy, R.; Beyeh, N. K. Host-Guest Interactions of Sodiumsulfonatomethyleneresorcinarene and Quaternary Ammonium Halides: An Experimental-Computational Analysis of the Guest Inclusion Properties. *Cryst. Growth Des.* **2020**, *20* (4), 2367–2376. https://doi.org/10.1021/acs.cgd.9b01540.

(3) Kobayashi, K.; Asakawa, Y.; Kato, Y.; Aoyama, Y. Complexation of Hydrophobic Sugars and Nucleosides in Water with Tetrasulfonate Derivatives of Resorcinol Cyclic Tetramer Having a Polyhydroxy Aromatic Cavity: Importance of Guest-Host CH-.Pi. Interaction. *J. Am. Chem. Soc.* **2002**, *114* (26), 10307–10313. https://doi.org/10.1021/JA00052A030.

(4) Kaiser, C. J. O.; Peters, C.; Schmid, P. W. N.; Stavropoulou, M.; Zou, J.; Dahiya, V.; Mymrikov, E. V.; Rockel, B.; Asami, S.; Haslbeck, M.; Rappsilber, J.; Reif, B.; Zacharias, M.; Buchner, J.; Weinkauf, S. The Structure and Oxidation of the Eye Lens Chaperone AA-Crystallin. *Nat. Struct. Mol. Biol.* **2019**, *26* (12), 1141–1150. https://doi.org/10.1038/s41594-019-0332-9.

(5) Pettersen, E. F.; Goddard, T. D.; Huang, C. C.; Couch, G. S.; Greenblatt, D. M.; Meng, E. C.; Ferrin, T. E. UCSF Chimera - A Visualization System for Exploratory Research and Analysis. *J. Comput. Chem.* **2004**, *25* (13), 1605–1612. https://doi.org/10.1002/jcc.20084.

(6) Frisch, M. J.; Trucks, G. W.; Schlegel, H. B.; Scuseria, G. E.; Robb, M. A.; Cheeseman, J. R.; Scalmani, G.; Barone, V.; Mennucci, B.; Petersson, G. A.; Nakatsuji, H.; Caricato, M.; Li, X.; Hratchian, H. P.; Izmaylov, A. F.; Bloino, J.; Zheng, G.; Sonnenberg, J. L.; Hada, M.; Ehara, M.; Toyota, K.; Fukuda, R.; Hasegawa, J.; Ishida, M.; Nakajima, T.; Honda, Y.; Kitao, O.; Nakai, H.; Vreven, T.; Montgomery Jr., J. A.; Peralta, J. E.; Ogliaro, F.; Bearpark, M.; Heyd, J. J.; Brothers, E.; Kudin, K. N.; Staroverov, V. N.; Kobayashi, R.; Normand, J.; Raghavachari, K.; Rendell, A.; Burant, J. C.; Iyengar, S. S.; Tomasi, J.; Cossi, M.; Rega, N.; Millam, J. M.; Klene, M.; Knox, J. E.; Cross, J. B.; Bakken, V.; Adamo, C.; Jaramillo, J.; Gomperts, R.; Stratmann, R. E.; Yazyev, O.; Austin, A. J.; Cammi, R.; Pomelli, C.; Ochterski, J. W.; Martin, R. L.; Morokuma, K.; Zakrzewski, V. G.; Voth, G. A.; Salvador, P.; Dannenberg, J. J.; Dapprich, S.; Daniels, A. D.; Farkas, J. B.; Foresman, J. B.; Ortiz, J. V; Cioslowski, J.; Fox, D. J. Gaussian09 Revision D.01, Gaussian Inc. Wallingford CT. *Gaussian 09 Revision C.01*. 2010, p Gaussian Inc., Wallingford CT.

(7) Beard, H.; Cholleti, A.; Pearlman, D.; Sherman, W.; Loving, K. A. Applying Physics-Based Scoring to Calculate Free Energies of Binding for Single Amino Acid Mutations in Protein-Protein Complexes. *PLoS One* **2013**, *8* (12), 82849. https://doi.org/10.1371/journal.pone.0082849.

(8) Gohlke, H.; Klebe, G. Approaches to the Description and Prediction of the Binding Affinity of Small-Molecule Ligands to Macromolecular Receptors. *Angew. Chem. Int. Ed.* **2002**, *41* (15), 2644–2676. https://doi.org/10.1002/1521-3773(20020802)41:15<2644::AID-ANIE2644>3.0.CO;2-O.